PERGAMON

International Journal of Solids and Structures 38 (2001) 4585–4608

INTERNATIONAL JOURNAL OF SOLIDS and STRUCTURES

www.elsevier.com/locate/ijsolstr

Asymptotic analysis of heterogeneous Cosserat media

Samuel Forest [a,*], Francis Pradel [b,1], Karam Sab [b,2]

[a] *Centre des Matériaux – UMR 7633, Ecole des Mines de Paris – CNRS, BP 87, 91003 Evry, France*

[b] *Ecole Nationale des Ponts et Chaussées, CERMMO, 6 et 8 Avenue Blaise Pascal, Cité Descartes, Champs-sur-Marne, 77455 Marne-la-Vallée Cedex 2, France*

Received 27 September 1999; in revised form 20 July 2000

Abstract

The present work deals with the development of homogenization procedures for periodic heterogeneous linear elastic Cosserat media. It is resorted to asymptotic methods classically used in periodic homogenization. It is shown that the nature of the homogeneous equivalent medium depends on the hierarchy of three characteristic lengths: the size l of the heterogeneities, the Cosserat intrinsic lengths l_c of the constituents and the typical size L of the considered structure. When l and l_c are comparable and much smaller than L, the effective medium is proved to be a Cauchy continuum with volume couples, whereas the case $l_c \sim L$ leads to a Cosserat effective medium. Finite element simulations are provided in the case of a fiber-matrix composite for a large range of characteristic lengths l_c and for two different volume fractions. Reference calculations involving every heterogeneity are compared to the response obtained using a homogeneous equivalent medium. The results confirm the predicted hierarchy of models and also show that a Cosserat effective medium still provide a good estimation when all characteristic lengths have the same order of magnitude.

Keywords: Heterogeneous materials; Cosserat continuum; Homogenization; Asymptotic methods; Metal-matrix composite; Finite element

1. Introduction

The non-linear effective properties of metal matrix composites can depend not only on the volume fraction of the particles and on their geometrical distribution in the matrix but also on their absolute size (Zhu et al., 1997). Classical homogenization methods can be used to account for the influence of the volume fraction, distribution and morphology of the particles (Sanchez-Palencia and Zaoui, 1985; Suquet, 1997), but they are not able to predict size effects in the mechanical behavior of heterogeneous materials. Zhu et al.

* Corresponding author. Tel.: +33-1-6076-3051; fax: +33-1-6076-3150.

E-mail address: samuel.forest@mat.ensmp.fr (S. Forest).

[1] Present address: Institut Français du Pétrole, 1 et 4 Avenue de Bois Preau, 92852 Rueil-Malmaison, France.

[2] Present address: LCPC, Point 23, 58 Boulevard Lefebvre, 75732 Paris Cedex 15, France.

0020-7683/01/$ - see front matter
PII: S0020-7683(00)00295-X

(1997) has proposed to incorporate intrinsic length scales in the constitutive behavior of the matrix. The authors use the strain gradient theory of plasticity (Aifantis, 1992) and examine the influence of a strain-gradient coefficient on the effective properties of a metal-matrix composite. In Besson et al. (1999), the matrix is regarded as a Cosserat material. For, several methods are available to incorporate some non-locality in the mechanical properties of the constituents of the heterogeneous material. The constitutive equations can be formulated in a fully non-local manner by introducing integro-differential equations. A perhaps more tractable way consists in enriching the continuum with higher-order gradients of the displacement field or with additional degrees of freedom (micro-rotations, micro-deformations, ...) (Eringen, 1976). Reasons for introducing generalized continuum models at the local level may be twofold. Firstly, it is a natural way to obtain an explicit dependence of the effective properties of composites or multiphase materials on the absolute size of the constituents with a continuum model and to account for size effects observed for instance in materials strengthened by inclusions, fibers or precipitates (Ashby, 1971). On the other hand, generalized continua can be used to limit strain localization phenomena that may occur in one constituent when it exhibits a strain softening behavior, as advocated by Besson et al. (1999). If the constituents of a heterogeneous material are described by a generalized continuum like second grade, Cosserat or micro-morphic media, specific homogenization methods must be designed to derive the effective properties of the material. The questions are the following: Does a homogeneous substitute medium exist? Under which conditions does it still have a non-local character? What is the relation between the effective characteristic length and that of the constituents? Bounds and estimates of the overall properties of heterogeneous linear couple stress media have already been proposed by Smyshlyaev and Fleck (1994). The results have been applied to another class of materials exhibiting size effects, namely random materials like polycrystals with grain size effects (Smyshlyaev and Fleck, 1996; Dai and Parks, 1998; Forest et al., 2000). Although most physically relevant applications deal with plasticity or damage phenomena, a first step is to develop homogenization methods for generalized continua in the case of linear elasticity (Smyshlaev and Fleck, 1994; Forest et al., 1999). These methods can then be applied to non-linear behavior by introducing some linear comparison solids.

In this work, the attention is focused on the case of heterogeneous Cosserat media with periodic microstructure. For that purpose, asymptotic methods classically used for periodic heterogeneous materials (Sanchez-Palencia, 1974) are applied to linear elastic Cosserat constituents. The main interest of asymptotic methods in homogenization theory lies in the fact that it can provide the form of the balance and constitutive equations of an effective medium without any assumption on their nature and form. In particular, the nature of the effective medium for a mixture of Cosserat media will not be assumed a priori but rather will be the major result of the asymptotic analysis. Asymptotic methods have been recently used by Gambin and Kröner (1989), Triantafyllidis and Bardenhagen (1996) and Boutin (1996) to get solutions of higher orders to the problem of the effective properties of periodic heterogeneous classical media. In contrast, the present analysis is restricted to the first orders in the asymptotic developments but the method is applied to the case of periodic heterogeneous Cosserat media. It will appear that two different homogenization schemes can be defined depending on the ratio of the size l of the unit cell to the characteristic length l_c of the Cosserat constituents (Forest and Sab, 1998). The homogenization schemes are finally applied to a periodic linear elastic fiber matrix composite. The effective properties are determined for a large spectrum of characteristic lengths l_c of the matrix and for two different fiber volume fractions. The quality of the effective medium found according to each homogenization scheme is assessed using structural computations: Cosserat simple glide and shear-flexion tests on a heterogeneous periodic structure are successively analyzed using the finite-element method.

A wide use of the nabla operator $\underline{\nabla}$ is made in the sequel. The notation used for the gradient and divergence operators are the following:

$$a\underline{\nabla} = a_{,i}\underline{\mathbf{e}}_i, \qquad \underline{\mathbf{a}} \otimes \underline{\nabla} = a_{i,j}\,\underline{\mathbf{e}}_i \otimes \underline{\mathbf{e}}_j, \qquad \underset{\sim}{\mathbf{a}} \cdot \underline{\nabla} = a_{ij,j}\,\underline{\mathbf{e}}_i,$$

where a, $\underset{\sim}{\mathbf{a}}$ and $\underset{\sim}{\underset{\sim}{\mathbf{a}}}$, respectively, denote a scalar, first- and second-rank tensors. The $(\underline{\mathbf{e}}_i)_{i=1,2,3}$ are the vectors of an orthonormal basis of space and the associated Cartesian coordinates have been used. Third- and fourth-rank tensors are, respectively, denoted by $\underset{\simeq}{\mathbf{a}}$ (or $\underset{\simeq}{\mathbf{a}}$) and $\underset{\approx}{\mathbf{a}}$. Indices can be contracted as follows:

$$\underset{\sim}{\mathbf{a}} : \underset{\sim}{\mathbf{b}} = a_{ij}b_{ij}, \qquad \underset{\simeq}{\mathbf{a}} : \underset{\sim}{\mathbf{b}} = a_{ijk}b_{jk}\underline{\mathbf{e}}_i, \qquad \underset{\approx}{\mathbf{a}} : \underset{\sim}{\mathbf{b}} = a_{ijkl}b_{kl}\underline{\mathbf{e}}_i \otimes \underline{\mathbf{e}}_j, \qquad \underset{\sim}{\mathbf{a}} : \underset{\approx}{\mathbf{A}} : \underset{\sim}{\mathbf{b}} = a_{ij}A_{ijkl}b_{kl}.$$

The third-rank permutation tensor reads $\underset{\simeq}{\boldsymbol{\epsilon}}$ (or $\underset{\simeq}{\epsilon}$), its component ϵ_{ijk} is the signature of permutation (i,j,k): $\epsilon_{ijk} = 1$ for an even permutation of $(1,2,3)$, -1 for an odd permutation and 0 otherwise. A skew-symmetric tensor $\underset{\sim}{\mathbf{a}}$ can be represented by the (pseudo-) vector $\underline{\mathbf{a}}$:

$$\underline{\mathbf{a}} = -\tfrac{1}{2}\underset{\simeq}{\boldsymbol{\epsilon}} : \underset{\sim}{\mathbf{a}}, \qquad \underset{\sim}{\mathbf{a}} = -\underset{\simeq}{\boldsymbol{\epsilon}} \cdot \underline{\mathbf{a}}.$$

The following relations then hold for the vector product:

$$\underline{\mathbf{a}} \times \underline{\mathbf{b}} = \underset{\simeq}{\boldsymbol{\epsilon}} : (\underline{\mathbf{a}} \otimes \underline{\mathbf{b}}) = \underset{\sim}{\mathbf{a}} \cdot \underline{\mathbf{b}} = -\underset{\sim}{\mathbf{b}} \cdot \underline{\mathbf{a}}.$$

If $\underset{\sim}{\mathbf{a}}$ and $\underset{\sim}{\mathbf{b}}$ are skew-symmetric

$$\underset{\sim}{\mathbf{a}} : \underset{\sim}{\mathbf{b}} = 2\underline{\mathbf{a}} \cdot \underline{\mathbf{b}}.$$

A rotation tensor $\underset{\sim}{\mathbf{R}}$ can be represented by a rotation vector $\underline{\boldsymbol{\Phi}}$ such that

$$\underset{\sim}{\mathbf{R}} = \underset{\sim}{\mathbf{1}} - \underset{\simeq}{\boldsymbol{\epsilon}} \cdot \underline{\boldsymbol{\Phi}} \quad \text{or} \quad \underline{\boldsymbol{\Phi}} = -\tfrac{1}{2}\underset{\simeq}{\boldsymbol{\epsilon}} : \underset{\sim}{\mathbf{R}}$$

in the case of small rotations.

2. Mechanics of periodic Cosserat media

2.1. Presentation of the Cosserat continuum

The motion of a Cosserat body Ω is described by two independent sets of degrees of freedom: the displacement $\underline{\mathbf{u}}$ and the micro-rotation $\underline{\boldsymbol{\phi}}$ attributed to each material points. The micro-rotation accounts for the rotation of a triad associated with an underlying micro-structure (Eringen, 1976). The associated deformation fields are the Cosserat deformation tensor $\underset{\sim}{\mathbf{e}}$ and the torsion-curvature tensor $\underset{\sim}{\boldsymbol{\kappa}}$ defined by

$$\underset{\sim}{\mathbf{e}} = \underline{\mathbf{u}} \otimes \underline{\nabla} + \underset{\simeq}{\boldsymbol{\epsilon}} \cdot \underline{\boldsymbol{\phi}}, \qquad \underset{\sim}{\boldsymbol{\kappa}} = \underline{\boldsymbol{\phi}} \otimes \underline{\nabla}. \tag{1}$$

The symmetric part of $\underset{\sim}{\mathbf{e}}$ corresponds to the usual strain tensor, whereas its skew-symmetric part accounts for the relative rotation of the material with respect to micro-structure. In this work, the analysis is restricted to small deformations, small micro-rotations and small curvatures. The statics of the Cosserat continuum is described by the generally non-symmetric force-stress tensor $\underset{\sim}{\boldsymbol{\sigma}}$ and the generally non-symmetric couple-stress tensor $\underset{\sim}{\boldsymbol{\mu}}$. These tensors must fulfill the local form of the balance equations in the static case for given body forces $\underline{\mathbf{f}}$ and body couples $\underline{\mathbf{c}}$:

$$\underset{\sim}{\boldsymbol{\sigma}} \cdot \underline{\nabla} + \underline{\mathbf{f}} = 0, \qquad \underset{\sim}{\boldsymbol{\mu}} \cdot \underline{\nabla} - \underset{\simeq}{\boldsymbol{\epsilon}} : \underset{\sim}{\boldsymbol{\sigma}} + \underline{\mathbf{c}} = 0 \quad \text{on } \Omega. \tag{2}$$

The constitutive equations for linear elastic centro-symmetric Cosserat materials read:

$$\underset{\sim}{\boldsymbol{\sigma}} = \underset{\approx}{\mathbf{a}} : \underset{\sim}{\mathbf{e}}, \qquad \underset{\sim}{\boldsymbol{\mu}} = \underset{\approx}{\mathbf{c}} : \underset{\sim}{\boldsymbol{\kappa}}. \tag{3}$$

The elasticity tensors display the major symmetries:

$$a_{ijkl} = a_{klij}, \quad c_{ijkl} = c_{klij}. \tag{4}$$

When the material does not admit point symmetry in its symmetry group, a coupling term arises between deformation and curvature in the previous constitutive equations. This is excluded here for the sake of simplicity. The setting of the boundary value problem on body Ω is then closed by the boundary conditions. In the following, we consider Dirichlet boundary conditions of the form:

$$\underline{\mathbf{u}}(\underline{\mathbf{x}}) = 0, \quad \underline{\boldsymbol{\phi}}(\underline{\mathbf{x}}) = 0 \qquad \forall \underline{\mathbf{x}} \in \partial\Omega, \tag{5}$$

where $\partial\Omega$ denote the boundary of Ω. Eqs. (1)–(3) and (5) define the boundary value problem $\mathscr{P}$.

The next sections of this work are restricted to Cosserat materials with periodic micro-structure. The heterogeneous material is then obtained by space tesselation with cells translated from a single cell Y^l. The period of the micro-structure is described by three dimensionless independent vectors $(\underline{\mathbf{a}}_1, \underline{\mathbf{a}}_2, \underline{\mathbf{a}}_3)$ such that

$$Y^l = \left\{ \underline{\mathbf{x}} = x_i \underline{\mathbf{a}}_i, \ |x_i| < \frac{l}{2} \right\},$$

where l is the characteristic size of the cell. We call $\underset{\approx}{\mathbf{a}}^l$ and $\underset{\approx}{\mathbf{c}}^l$, the elasticity tensor fields of the periodic Cosserat material. They are such that

$$\forall \underline{\mathbf{x}} \in \Omega, \quad \forall (n_1, n_2, n_3) \in Z^3 \quad \underline{\mathbf{x}} + l(n_1\underline{\mathbf{a}}_1 + n_2\underline{\mathbf{a}}_2 + n_3\underline{\mathbf{a}}_3) \in \Omega$$

$$\underset{\approx}{\mathbf{a}}^l(\underline{\mathbf{x}}) = \underset{\approx}{\mathbf{a}}^l(\underline{\mathbf{x}} + l(n_1\underline{\mathbf{a}}_1 + n_2\underline{\mathbf{a}}_2 + n_3\underline{\mathbf{a}}_3)), \qquad \underset{\approx}{\mathbf{c}}^l(\underline{\mathbf{x}}) = \underset{\approx}{\mathbf{c}}^l(\underline{\mathbf{x}} + l(n_1\underline{\mathbf{a}}_1 + n_2\underline{\mathbf{a}}_2 + n_3\underline{\mathbf{a}}_3)).$$

2.2. Dimensional analysis

The diameter L of body Ω is defined as the maximum distance between two points:

$$L = \max_{(\underline{\mathbf{x}},\underline{\mathbf{y}}) \in \Omega \times \Omega} |\underline{\mathbf{x}} - \underline{\mathbf{y}}|.$$

Dimensionless coordinates and displacements can be introduced,

$$\underline{\mathbf{x}}^* = \frac{\underline{\mathbf{x}}}{L}, \qquad \underline{\mathbf{u}}^*(\underline{\mathbf{x}}^*) = \frac{\underline{\mathbf{u}}(\underline{\mathbf{x}})}{L}, \qquad \underline{\boldsymbol{\phi}}^*(\underline{\mathbf{x}}^*) = \underline{\boldsymbol{\phi}}(\underline{\mathbf{x}}). \tag{6}$$

The corresponding strain measures are

$$\underset{\sim}{\mathbf{e}}^*(\underline{\mathbf{x}}^*) = \underline{\mathbf{u}}^* \otimes \underline{\nabla}^* + \underset{\approx}{\boldsymbol{\epsilon}} \cdot \underline{\boldsymbol{\phi}}^* = \underset{\sim}{\mathbf{e}}(\underline{\mathbf{x}}), \qquad \underset{\sim}{\boldsymbol{\kappa}}^*(\underline{\mathbf{x}}^*) = \underline{\boldsymbol{\phi}}^* \otimes \underline{\nabla}^* = L\underset{\sim}{\boldsymbol{\kappa}}(\underline{\mathbf{x}}) \tag{7}$$

with $\underline{\nabla}^* = (\partial \cdot / \partial x_i^*)\,\underline{\mathbf{e}}_i$. It is necessary to introduce next a norm of the elasticity tensors:

$$A = \max_{\underline{\mathbf{x}} \in Y^l} \left| a^l_{ijkl}(\underline{\mathbf{x}}) \right|, \qquad C = \max_{\underline{\mathbf{x}} \in Y^l} \left| c^l_{ijkl}(\underline{\mathbf{x}}) \right| \tag{8}$$

whereby a characteristic length l_c can be defined

$$C = A l_c^2. \tag{9}$$

The definition of dimensionless stress and elasticity tensors follows:

$$\underset{\sim}{\boldsymbol{\sigma}}^*(\underline{\mathbf{x}}^*) = A^{-1}\underset{\sim}{\boldsymbol{\sigma}}(\underline{\mathbf{x}}), \qquad \underset{\sim}{\boldsymbol{\mu}}^*(\underline{\mathbf{x}}^*) = (AL)^{-1}\underset{\sim}{\boldsymbol{\mu}}(\underline{\mathbf{x}}), \tag{10}$$

$$\underset{\approx}{\mathbf{a}}^*(\underline{\mathbf{x}}^*) = A^{-1}\underset{\approx}{\mathbf{a}}^l(\underline{\mathbf{x}}), \qquad \underset{\approx}{\mathbf{c}}^*(\underline{\mathbf{x}}^*) = (Al_c^2)^{-1}\underset{\approx}{\mathbf{c}}^l(\underline{\mathbf{x}}). \tag{11}$$

Since the initial tensors $\underset{\approx}{\mathbf{a}}^l$ and $\underset{\approx}{\mathbf{c}}^l$ are Y^l-periodic, the dimensionless counterparts are Y^*-periodic:

$$Y^* = \frac{l}{L} Y, \qquad Y = \left\{ \underline{\mathbf{y}} = y_i \underline{\mathbf{a}}_i, \ |y_i| < \tfrac{1}{2} \right\}. \tag{12}$$

Y is the (dimensionless) unit cell used in the present asymptotic analyses. As a result, the dimensionless stress and strain tensors are related by the following constitutive equations:

$$\underset{\sim}{\boldsymbol{\sigma}}^* = \underset{\approx}{\mathbf{a}}^* : \underset{\sim}{\mathbf{e}}^*, \quad \underset{\sim}{\boldsymbol{\mu}}^* = \left(\frac{l_c}{L} \right)^2 \underset{\approx}{\mathbf{c}}^* : \underset{\sim}{\boldsymbol{\kappa}}^*. \tag{13}$$

The dimensionless balance equations read

$$\forall \underline{\mathbf{x}}^* \in \Omega^*, \quad \underset{\sim}{\boldsymbol{\sigma}}^* \cdot \underline{\nabla}^* + \underline{\mathbf{f}}^* = 0, \qquad \underset{\sim}{\boldsymbol{\mu}}^* \cdot \underline{\nabla}^* - \underset{\simeq}{\boldsymbol{\epsilon}} : \underset{\sim}{\boldsymbol{\sigma}}^* + \underline{\mathbf{c}}^* = 0 \tag{14}$$

with $\underline{\mathbf{f}}^*(\underline{\mathbf{x}}^*) = LA^{-1}\underline{\mathbf{f}}(\underline{\mathbf{x}})$ and $\underline{\mathbf{c}}^*(\underline{\mathbf{x}}^*) = A^{-1}\underline{\mathbf{c}}(\underline{\mathbf{x}})$. A boundary value problem $\mathscr{P}^*$ can be defined using Eqs. (7), (13) and (14), complemented by the boundary conditions:

$$\forall \underline{\mathbf{x}}^* \in \partial\Omega^*, \qquad \underline{\mathbf{u}}^*(\underline{\mathbf{x}}^*) = 0, \quad \underline{\boldsymbol{\phi}}^*(\underline{\mathbf{x}}^*) = 0. \tag{15}$$

3. Asymptotic analysis of Cosserat media

3.1. The homogenization problem

The boundary value problem $\mathscr{P}^*$ is treated here as an element of a series of problems $(\mathscr{P}_\varepsilon)_{\varepsilon>0}$ on Ω^*. The homogenization problem consists in the determination of the limit of this series when the dimensionless parameter ε, regarded as small, tends towards 0. The series is chosen such that

$$\mathscr{P}_{\varepsilon=l/L} = \mathscr{P}^*.$$

The unknowns of boundary value problem $\mathscr{P}_\varepsilon$ are the displacement and micro-rotation fields $\underline{\mathbf{u}}^\varepsilon$ and $\underline{\boldsymbol{\phi}}^\varepsilon$ satisfying the following field equations on Ω^*:

$$\underset{\sim}{\boldsymbol{\sigma}}^\varepsilon = \underset{\approx}{\mathbf{a}}^\varepsilon : (\underline{\mathbf{u}}^\varepsilon \otimes \underline{\nabla}^* + \underset{\simeq}{\boldsymbol{\epsilon}} : \underline{\boldsymbol{\phi}}^\varepsilon), \qquad \underset{\sim}{\boldsymbol{\mu}}^\varepsilon = \underset{\approx}{\mathbf{c}}^\varepsilon : (\underline{\boldsymbol{\phi}}^\varepsilon \otimes \underline{\nabla}^*),$$

$$\underset{\sim}{\boldsymbol{\sigma}}^\varepsilon \cdot \underline{\nabla}^* + \underline{\mathbf{f}}^\varepsilon, \qquad \underset{\sim}{\boldsymbol{\mu}}^\varepsilon \cdot \underline{\nabla}^* - \underset{\simeq}{\boldsymbol{\epsilon}} : \underset{\sim}{\boldsymbol{\sigma}}^\varepsilon + \underline{\mathbf{c}}^\varepsilon = 0.$$

Regarding body forces and couples, we take

$$\underline{\mathbf{f}}^\varepsilon(\underline{\mathbf{x}}^*) = \underline{\mathbf{f}}^*(\underline{\mathbf{x}}^*), \quad \underline{\mathbf{c}}^\varepsilon(\underline{\mathbf{x}}^*) = \underline{\mathbf{c}}^*(\underline{\mathbf{x}}^*) \qquad \forall \varepsilon > 0. \tag{16}$$

Different cases must now be distinguished depending on the relative position of the constitutive length l_c with respect to the characteristic lengths l and L of the problem. Two special cases are relevant for the present asymptotic analysis. The first case corresponds to a limiting process for which l_c/l remains constant when l/L goes to zero. The second case corresponds to the situation for which l_c/L remains constant when l/L goes to zero. These assumptions lead to two different homogenization schemes labelled HS1 and HS2 in the sequel. HS1 (resp. 2) will be relevant when the ratio l/L is small enough and when l_c and l (resp. L) have the same order of magnitude, as indicated in Fig. 1. The two shaded regions of Fig. 1 correspond to $l_c/l \sim 1$ (or smaller) and $l_c/L \sim 1$.

Accordingly, the three following tensors of elastic moduli can be defined:

$$\underset{\approx}{\mathbf{a}}^{(0)}(\underline{\mathbf{y}}) = \underset{\approx}{\mathbf{a}}^*\left(\frac{l}{L}\underline{\mathbf{y}} \right), \qquad \underset{\approx}{\mathbf{c}}^{(1)}(\underline{\mathbf{y}}) = \left(\frac{l_c}{l} \right)^2 \underset{\approx}{\mathbf{c}}^*\left(\frac{l}{L}\underline{\mathbf{y}} \right), \qquad \underset{\approx}{\mathbf{c}}^{(2)}(\underline{\mathbf{y}}) = \left(\frac{l_c}{L} \right)^2 \underset{\approx}{\mathbf{c}}^*\left(\frac{l}{L}\underline{\mathbf{y}} \right). \tag{17}$$

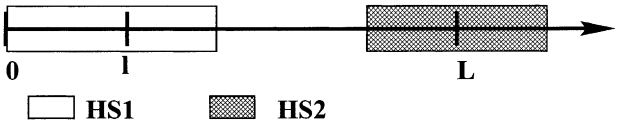

Fig. 1. Range of possible variation of intrinsic length l_c with respect to the characteristic lengths of the problem for the homogenization problems considered in this work.

They are Y-periodic since $\underset{\approx}{\mathbf{a}}^*$ and $\underset{\approx}{\mathbf{c}}^*$ are Y^*-periodic. Two different hypotheses will be made concerning the constitutive tensors of problem $\mathscr{P}_\varepsilon$:

Assumption 1. $\underset{\approx}{\mathbf{a}}^\varepsilon(\underline{\mathbf{x}}^*) = \underset{\approx}{\mathbf{a}}^{(0)}(\varepsilon^{-1}\underline{\mathbf{x}}^*)$ and $\underset{\approx}{\mathbf{c}}^\varepsilon(\underline{\mathbf{x}}^*) = \varepsilon^2\underset{\approx}{\mathbf{c}}^{(1)}(\varepsilon^{-1}\underline{\mathbf{x}}^*)$.

Assumption 2. $\underset{\approx}{\mathbf{a}}^\varepsilon(\underline{\mathbf{x}}^*) = \underset{\approx}{\mathbf{a}}^{(0)}(\varepsilon^{-1}\underline{\mathbf{x}}^*)$ and $\underset{\approx}{\mathbf{c}}^\varepsilon(\underline{\mathbf{x}}^*) = \underset{\approx}{\mathbf{c}}^{(2)}(\varepsilon^{-1}\underline{\mathbf{x}}^*)$.

Assumptions 1 and 2, respectively, correspond to the homogenization schemes, HS1 and HS2. Both choices meet the requirement that

$$\left(\varepsilon = \frac{l}{L}\right) \Rightarrow \left(\underset{\approx}{\mathbf{a}}^\varepsilon = \underset{\approx}{\mathbf{a}}^*, \qquad \underset{\approx}{\mathbf{c}}^\varepsilon = \left(\frac{l_c}{L}\right)^2 \underset{\approx}{\mathbf{c}}^*\right).$$

It must be noted that, in our presentation of the asymptotic analysis, the lengths l, l_c and L are given and fixed, whereas parameter ε is allowed to tend to zero in the limiting process. HS1 and HS2 are summarized in Table 1. In Table 1 and in the sequel, the asterisks are dropped for conciseness.

3.2. Multiscale asymptotic method

In the setting of the homogenization problems, two space variables have been distinguished: $\underline{\mathbf{x}}$ describes the macroscopic scale and $\underline{\mathbf{y}}$ is the local variable in the unit cell Y. To solve the homogenization problem settled in Table 1, it is resorted to the method of multiscale asymptotic developments initially introduced by Sanchez-Palencia (1974). According to this method, all fields are regarded as functions of the two variables $\underline{\mathbf{x}}$ and $\underline{\mathbf{y}}$, and it is assumed that they can be expanded in a series of powers of small parameter ε. In particular, the displacement, micro-rotation, force and couple stress fields are supposed to take the form:

Table 1
Equations of boundary value problem $\mathscr{P}_\varepsilon$ including the assumptions of the two homogenization schemes presented in this work (see Section 3.1, the asterisks have been dropped for simplicity)

Homogenization problems
Boundary conditions on $\partial\Omega$: $\underline{\mathbf{u}}^\varepsilon(\underline{\mathbf{x}}) = 0$ and $\underline{\boldsymbol{\phi}}^\varepsilon(\underline{\mathbf{x}}) = 0,\ \forall \underline{\mathbf{x}} \in \partial\Omega$
Volume forces and couples: $\underline{\mathbf{f}}^\varepsilon(\underline{\mathbf{x}}) = \underline{\mathbf{f}}(\underline{\mathbf{x}})$ and $\underline{\mathbf{c}}^\varepsilon(\underline{\mathbf{x}}) = \underline{\mathbf{c}}(\underline{\mathbf{x}})$
Balance equations: $\underset{\sim}{\boldsymbol{\sigma}}^\varepsilon \cdot \underline{\nabla} + \underline{\mathbf{f}} = 0$ and $\underset{\sim}{\boldsymbol{\mu}}^\varepsilon \cdot \underline{\nabla} - \underset{\approx}{\boldsymbol{\epsilon}} : \underset{\sim}{\boldsymbol{\sigma}}^\varepsilon + \underline{\mathbf{c}} = 0,\ \forall \underline{\mathbf{x}} \in \Omega$
Kinematics: $\underset{\sim}{\mathbf{e}}^\varepsilon = \underline{\mathbf{u}}^\varepsilon \otimes \underline{\nabla} + \underset{\approx}{\boldsymbol{\epsilon}}.\underline{\boldsymbol{\phi}}^\varepsilon$ and $\underset{\sim}{\boldsymbol{\kappa}}^\varepsilon = \underline{\boldsymbol{\phi}}^\varepsilon \otimes \underline{\nabla}$
Consitutive equations: $\underset{\sim}{\boldsymbol{\sigma}}^\varepsilon = \underset{\approx}{\mathbf{a}}^\varepsilon : \underset{\sim}{\mathbf{e}}^\varepsilon$ and $\underset{\sim}{\boldsymbol{\mu}}^\varepsilon = \underset{\approx}{\mathbf{c}}^\varepsilon : \underset{\sim}{\boldsymbol{\kappa}}^\varepsilon$
(i) First scheme (HS1)
$\underset{\approx}{\mathbf{a}}^\varepsilon(\underline{\mathbf{x}}) = \underset{\approx}{\mathbf{a}}^{(0)}(\underline{\mathbf{y}})$
$\underset{\approx}{\mathbf{c}}^\varepsilon(\underline{\mathbf{x}}) = \varepsilon^2\underset{\approx}{\mathbf{c}}^{(1)}(\underline{\mathbf{y}})$
(ii) Second scheme (HS2)
$\underset{\approx}{\mathbf{a}}^\varepsilon(\underline{\mathbf{x}}) = \underset{\approx}{\mathbf{a}}^{(0)}(\underline{\mathbf{y}})$
$\underset{\approx}{\mathbf{c}}^\varepsilon(\underline{\mathbf{x}}) = \underset{\approx}{\mathbf{c}}^{(2)}(\underline{\mathbf{y}})$
where $\underline{\mathbf{y}} = \underline{\mathbf{x}}/\varepsilon$ and $\underset{\approx}{\mathbf{a}}^{(0)}, \underset{\approx}{\mathbf{c}}^{(1)}$ and $\underset{\approx}{\mathbf{c}}^{(2)}$ are Y-periodic

$$\begin{aligned}
\underline{\mathbf{u}}^{\varepsilon}(\underline{\mathbf{x}}) &= \underline{\mathbf{u}}_0(\underline{\mathbf{x}},\underline{\mathbf{y}}) + \varepsilon\underline{\mathbf{u}}_1(\underline{\mathbf{x}},\underline{\mathbf{y}}) + \varepsilon^2\underline{\mathbf{u}}_2(\underline{\mathbf{x}},\underline{\mathbf{y}}) + \cdots,\\
\underline{\boldsymbol{\phi}}^{\varepsilon}(\underline{\mathbf{x}}) &= \underline{\boldsymbol{\phi}}_1(\underline{\mathbf{x}},\underline{\mathbf{y}}) + \varepsilon\underline{\boldsymbol{\phi}}_2(\underline{\mathbf{x}},\underline{\mathbf{y}}) + \varepsilon^2\underline{\boldsymbol{\phi}}_3(\underline{\mathbf{x}},\underline{\mathbf{y}}) + \cdots,\\
\underset{\sim}{\boldsymbol{\sigma}}^{\varepsilon} &= \underset{\sim}{\boldsymbol{\sigma}}_0(\underline{\mathbf{x}},\underline{\mathbf{y}}) + \varepsilon\underset{\sim}{\boldsymbol{\sigma}}_1(x,y) + \cdots,\\
\underset{\sim}{\boldsymbol{\mu}}^{\varepsilon} &= \underset{\sim}{\boldsymbol{\mu}}_0(\underline{\mathbf{x}},\underline{\mathbf{y}}) + \varepsilon\underset{\sim}{\boldsymbol{\mu}}_1(x,y) + \cdots,
\end{aligned} \tag{18}$$

where the $\underline{\mathbf{u}}_i(\underline{\mathbf{x}},\underline{\mathbf{y}})$, $\underline{\boldsymbol{\phi}}_i(\underline{\mathbf{x}},\underline{\mathbf{y}})$, $\underset{\sim}{\boldsymbol{\sigma}}_i(\underline{\mathbf{x}},\underline{\mathbf{y}})$ and $\underset{\sim}{\boldsymbol{\mu}}_i(\underline{\mathbf{x}},\underline{\mathbf{y}})$ coefficients are assumed to have the same order of magnitude and to be Y-periodic with respect to variable $\underline{\mathbf{y}}$ ($\underline{\mathbf{y}} = \underline{\mathbf{x}}/\varepsilon$). The average operator over the unit cell Y is denoted by

$$\langle\cdot\rangle = \frac{1}{|Y|}\int_Y \cdot\, \mathrm{d}\omega_y.$$

As a result,

$$\langle\underline{\mathbf{u}}^{\varepsilon}\rangle = \underline{\mathbf{U}}_0 + \varepsilon\underline{\mathbf{U}}_1 + \cdots, \qquad \langle\underline{\boldsymbol{\phi}}^{\varepsilon}\rangle = \underline{\boldsymbol{\Phi}}_1 + \varepsilon\underline{\boldsymbol{\Phi}}_2 + \cdots, \tag{19}$$

where $\underline{\mathbf{U}}_i = \langle\underline{\mathbf{u}}_i\rangle$ and $\underline{\boldsymbol{\Phi}}_i = \langle\underline{\boldsymbol{\phi}}_i\rangle$. The gradient operator can be split into partial derivatives with respect to $\underline{\mathbf{x}}$ and $\underline{\mathbf{y}}$:

$$\underline{\boldsymbol{\nabla}} = \underline{\boldsymbol{\nabla}}_x + \frac{1}{\varepsilon}\underline{\boldsymbol{\nabla}}_y. \tag{20}$$

This operator is used to compute the Cosserat strain measures and balance equations:

$$\begin{aligned}
\underset{\sim}{\mathbf{e}}^{\varepsilon} &= \varepsilon^{-1}\underset{\sim}{\mathbf{e}}_{-1} + \underset{\sim}{\mathbf{e}}_0 + \varepsilon^1\underset{\sim}{\mathbf{e}}_1 + \cdots\\
&= \varepsilon^{-1}\underline{\mathbf{u}}_0\otimes\underline{\boldsymbol{\nabla}}_y + (\underline{\mathbf{u}}_0\otimes\underline{\boldsymbol{\nabla}}_x + \underline{\mathbf{u}}_1\otimes\underline{\boldsymbol{\nabla}}_y + \underline{\underline{\boldsymbol{\epsilon}}}\cdot\underline{\boldsymbol{\phi}}_1) + \varepsilon(\underline{\mathbf{u}}_1\otimes\underline{\boldsymbol{\nabla}}_x + \underline{\mathbf{u}}_2\otimes\underline{\boldsymbol{\nabla}}_y + \underline{\underline{\boldsymbol{\epsilon}}}\cdot\underline{\boldsymbol{\phi}}_2) + \cdots,\\
\underset{\sim}{\boldsymbol{\kappa}}^{\varepsilon} &= \varepsilon^{-1}\underset{\sim}{\boldsymbol{\kappa}}_{-1} + \underset{\sim}{\boldsymbol{\kappa}}_0 + \varepsilon^1\underset{\sim}{\boldsymbol{\kappa}}_1 + \cdots\\
&= \varepsilon^{-1}\underline{\boldsymbol{\phi}}_1\otimes\underline{\boldsymbol{\nabla}}_y \ + (\underline{\boldsymbol{\phi}}_1\otimes\underline{\boldsymbol{\nabla}}_x + \underline{\boldsymbol{\phi}}_2\otimes\underline{\boldsymbol{\nabla}}_y) + \varepsilon(\underline{\boldsymbol{\phi}}_2\otimes\underline{\boldsymbol{\nabla}}_x + \underline{\boldsymbol{\phi}}_3\otimes\underline{\boldsymbol{\nabla}}_y) + \cdots,
\end{aligned} \tag{21}$$

$$\underset{\sim}{\boldsymbol{\sigma}}^{\varepsilon}\cdot\underline{\boldsymbol{\nabla}}_x + \varepsilon^{-1}\underset{\sim}{\boldsymbol{\sigma}}^{\varepsilon}\cdot\underline{\boldsymbol{\nabla}}_y + \underline{\mathbf{f}} = 0, \qquad \underset{\sim}{\boldsymbol{\mu}}^{\varepsilon}\cdot\underline{\boldsymbol{\nabla}}_x + \varepsilon^{-1}\underset{\sim}{\boldsymbol{\mu}}^{\varepsilon}\cdot\underline{\boldsymbol{\nabla}}_y - \underline{\underline{\boldsymbol{\epsilon}}} : \underset{\sim}{\boldsymbol{\sigma}}^{\varepsilon} + \underline{\mathbf{c}} = 0. \tag{22}$$

The expansions of the stress tensors are then introduced in the balance equations (22) and the terms can be ordered with respect to the powers of ε. Identifying the terms of same order, we are lead to the following set of equations:

- Order ε^{-1}

$$\underset{\sim}{\boldsymbol{\sigma}}_0\cdot\underline{\boldsymbol{\nabla}}_y = 0, \qquad \underset{\sim}{\boldsymbol{\mu}}_0\cdot\underline{\boldsymbol{\nabla}}_y = 0. \tag{23}$$

- Order ε^0

$$\underset{\sim}{\boldsymbol{\sigma}}_0\cdot\underline{\boldsymbol{\nabla}}_x + \underset{\sim}{\boldsymbol{\sigma}}_1\cdot\underline{\boldsymbol{\nabla}}_y + \underline{\mathbf{f}} = 0, \qquad \underset{\sim}{\boldsymbol{\mu}}_0\cdot\underline{\boldsymbol{\nabla}}_x + \underset{\sim}{\boldsymbol{\mu}}_1\cdot\underline{\boldsymbol{\nabla}}_y - \underline{\underline{\boldsymbol{\epsilon}}} : \underset{\sim}{\boldsymbol{\sigma}}_0 + \underline{\mathbf{c}} = 0. \tag{24}$$

The effective balance equations follow from Eqs. (23) and (24) by averaging over the unit cell Y and at the order ε^0, one gets

$$\underset{\sim}{\boldsymbol{\Sigma}}_0\cdot\underline{\boldsymbol{\nabla}} + \underline{\mathbf{f}} = 0, \qquad \underset{\sim}{\mathbf{M}}_0\cdot\underline{\boldsymbol{\nabla}} - \underline{\underline{\boldsymbol{\epsilon}}} : \underset{\sim}{\boldsymbol{\Sigma}}_0 + \underline{\mathbf{c}} = 0, \tag{25}$$

where $\underset{\sim}{\boldsymbol{\Sigma}}_0 = \langle\underset{\sim}{\boldsymbol{\sigma}}_0\rangle$ and $\underset{\sim}{\mathbf{M}}_0 = \langle\underset{\sim}{\boldsymbol{\mu}}_0\rangle$.

3.3. First homogenization scheme

For the HS1 defined in Section 3.2, the equations describing the local behavior are

$$\underset{\sim}{\boldsymbol{\sigma}}^{\varepsilon} = \underset{\approx}{\mathbf{a}}^{(0)}(\underline{\mathbf{y}}) : \underset{\sim}{\mathbf{e}}^{\varepsilon}, \qquad \underset{\sim}{\boldsymbol{\mu}}^{\varepsilon} = \varepsilon^2 \underset{\approx}{\mathbf{c}}^{(1)}(\underline{\mathbf{y}}) : \underset{\sim}{\boldsymbol{\kappa}}^{\varepsilon}. \tag{26}$$

At this stage, the expansion (21) can be substituted into the constitutive equations (26). Identifying the terms of same order, we get

- Order ε^{-1}

$$\underset{\approx}{\mathbf{a}}^{(0)} : \underset{\sim}{\mathbf{e}}_{-1} = \underset{\approx}{\mathbf{a}}^{(0)} : \underline{\mathbf{u}}_0 \otimes \underline{\boldsymbol{\nabla}}_y = 0. \tag{27}$$

- Order ε^0

$$\underset{\sim}{\boldsymbol{\sigma}}_0 = \underset{\approx}{\mathbf{a}}^{(0)} : \underset{\sim}{\mathbf{e}}_0, \qquad \underset{\sim}{\boldsymbol{\mu}}_0 = 0. \tag{28}$$

Eq. (27) implies that $\underline{\mathbf{u}}_0$ does not depend on the local variable $\underline{\mathbf{y}}$:

$$\underline{\mathbf{u}}_0(\underline{\mathbf{x}}, \underline{\mathbf{y}}) = \underline{\mathbf{U}}_0(\underline{\mathbf{x}}).$$

At order ε^0, the couple stresses vanish, so that

$$\underset{\sim}{\mathbf{M}}_0 = 0.$$

Finally, the fields $(\underline{\mathbf{u}}_1, \underline{\boldsymbol{\phi}}_1, \underset{\sim}{\boldsymbol{\sigma}}_0, \underset{\sim}{\boldsymbol{\mu}}_1)$ and $(\underline{\mathbf{u}}_2, \underline{\boldsymbol{\phi}}_2, \underset{\sim}{\boldsymbol{\sigma}}_1, \underset{\sim}{\boldsymbol{\mu}}_2)$ are solutions of the two following auxiliary boundary value problems defined on the unit cell:

$$\begin{cases} \underset{\sim}{\mathbf{e}}_0 = \underline{\mathbf{U}}_0 \otimes \underline{\boldsymbol{\nabla}}_x + \underline{\mathbf{u}}_1 \otimes \underline{\boldsymbol{\nabla}}_y + \underset{\approx}{\boldsymbol{\epsilon}} \cdot \underline{\boldsymbol{\phi}}_1, & \underset{\sim}{\boldsymbol{\kappa}}_{-1} = \underline{\boldsymbol{\phi}}_1 \otimes \underline{\boldsymbol{\nabla}}_y, \\ \underset{\sim}{\boldsymbol{\sigma}}_0 = \underset{\approx}{\mathbf{a}}^{(0)} : \underset{\sim}{\mathbf{e}}_0, & \underset{\sim}{\boldsymbol{\mu}}_1 = \underset{\approx}{\mathbf{c}}^{(1)} : \underset{\sim}{\boldsymbol{\kappa}}_{-1}, \\ \underset{\sim}{\boldsymbol{\sigma}}_0 \cdot \underline{\boldsymbol{\nabla}}_y = 0, & \underset{\sim}{\boldsymbol{\mu}}_1 \cdot \underline{\boldsymbol{\nabla}}_y - \underset{\approx}{\boldsymbol{\epsilon}} : \underset{\sim}{\boldsymbol{\sigma}}_0 + \underline{\mathbf{c}} = 0, \end{cases} \tag{29}$$

$$\begin{cases} \underset{\sim}{\mathbf{e}}_1 = \underline{\mathbf{u}}_1 \otimes \underline{\boldsymbol{\nabla}}_x + \underline{\mathbf{u}}_2 \otimes \underline{\boldsymbol{\nabla}}_y + \underset{\approx}{\boldsymbol{\epsilon}} \cdot \underline{\boldsymbol{\phi}}_2, & \underset{\sim}{\boldsymbol{\kappa}}_0 = \underline{\boldsymbol{\phi}}_1 \otimes \underline{\boldsymbol{\nabla}}_x + \underline{\boldsymbol{\phi}}_2 \otimes \underline{\boldsymbol{\nabla}}_y, \\ \underset{\sim}{\boldsymbol{\sigma}}_1 = \underset{\approx}{\mathbf{a}}^{(0)} : \underset{\sim}{\mathbf{e}}_1, & \underset{\sim}{\boldsymbol{\mu}}_2 = \underset{\approx}{\mathbf{c}}^{(1)} : \underset{\sim}{\boldsymbol{\kappa}}_0, \\ \underset{\sim}{\boldsymbol{\sigma}}_0 \cdot \underline{\boldsymbol{\nabla}}_x + \underset{\sim}{\boldsymbol{\sigma}}_1 \cdot \underline{\boldsymbol{\nabla}}_y + \underline{\mathbf{f}} = 0, & \underset{\sim}{\boldsymbol{\mu}}_1 \cdot \underline{\boldsymbol{\nabla}}_x + \underset{\sim}{\boldsymbol{\mu}}_2 \cdot \underline{\boldsymbol{\nabla}}_y - \underset{\approx}{\boldsymbol{\epsilon}} : \underset{\sim}{\boldsymbol{\sigma}}_1 = 0. \end{cases} \tag{30}$$

The boundary conditions of these problems are given by the periodicity requirements for the unknown fields. A series of auxiliary problems similar to Eq. (30) can be defined to obtain the solutions at higher orders. It must be noted that these problems must be solved in cascade since, for instance, the solution of Eq. (29) (resp. (30)) requires the knowledge of $\underline{\mathbf{U}}_0$ (resp. $\underline{\mathbf{u}}_1$ and $\underline{\boldsymbol{\phi}}_1$). The detailed resolution of problem (29) is presented in Appendix A, whereas a solution of problem (30) can be found in (Pradel, 1998). We simply remark here that the solution $(\underline{\mathbf{u}}_1, \underline{\boldsymbol{\phi}}_1 - \underline{\boldsymbol{\Omega}})$ to problem (29) is linear in $\underline{\mathbf{U}}_0 \overset{s}{\otimes} \underline{\boldsymbol{\nabla}}_x$ and $\underline{\mathbf{c}}$ up to a translation term, so that

$$\underline{\mathbf{u}}^{\varepsilon} = \underline{\mathbf{U}}_0(\underline{\mathbf{x}}) + \varepsilon(\underline{\mathbf{U}}_1(\underline{\mathbf{x}}) + \underset{\approx}{\boldsymbol{X}}_u^{(1)}(\underline{\mathbf{y}}) : \underline{\mathbf{U}}_0 \overset{s}{\otimes} \underline{\boldsymbol{\nabla}} + \underset{\sim}{\mathbf{T}}_u(\underline{\mathbf{y}}) \cdot \underline{\mathbf{c}}) + \cdots, \tag{31}$$

$$\underline{\boldsymbol{\phi}}^{\varepsilon} = \underline{\boldsymbol{\Omega}}(\underline{\mathbf{x}}) + \underset{\approx}{\boldsymbol{X}}_{\phi}^{(1)}(\underline{\mathbf{y}}) : \underline{\mathbf{U}}_0 \overset{s}{\otimes} \underline{\boldsymbol{\nabla}} + \underset{\sim}{\mathbf{T}}_{\phi}(\underline{\mathbf{y}}) \cdot \underline{\mathbf{c}} + \cdots, \tag{32}$$

where $\underline{\boldsymbol{\Omega}}$ is the vector associated to the skew-symmetric part of $\underline{\mathbf{U}}_0 \otimes \underline{\boldsymbol{\nabla}}$ and its symmetric part is $\underline{\mathbf{U}}_0 \overset{s}{\otimes} \underline{\boldsymbol{\nabla}}$. Concentration tensors $\underset{\approx}{\boldsymbol{X}}_{u,\phi}^{(1)}$ and $\underset{\sim}{\mathbf{T}}_{u,\phi}$ have been introduced, the components of which are given by the

successive solutions of the auxiliary problem for unit values of the components of $\underline{\mathbf{U}}_0 \overset{s}{\otimes} \underline{\nabla}$ and $\underline{\mathbf{c}}$. Concentration tensor $\underset{\approx}{\boldsymbol{X}}_u^{(1)}$ is such that its mean value over the unit cell vanishes.

Main results of the analysis

The main results of the first analysis are given by Eqs. (33)–(35). The effective medium turns out to be a Cauchy continuum with volume couples, described by the displacement field $\underline{\mathbf{U}}_0$ and governed by the following effective equations:

$$\underset{\sim}{\boldsymbol{\Sigma}}_0 = \underset{\approx}{\mathbf{A}}_0^{(1)} : \underline{\mathbf{U}}_0 \overset{s}{\otimes} \underline{\nabla} - \tfrac{1}{2} \underset{\approx}{\boldsymbol{\epsilon}} \cdot \underline{\mathbf{c}}, \tag{33}$$

$$\underset{\sim}{\boldsymbol{\Sigma}}_0 \cdot \underline{\nabla} + \underline{\mathbf{f}} = 0, \tag{34}$$

and the boundary conditions $\underline{\mathbf{U}}_0 = 0$ on $\partial\Omega$. The contribution of $\underline{\mathbf{c}}$ to $\underset{\sim}{\boldsymbol{\Sigma}}_0$ follows directly from the linearity of $\underset{\sim}{\boldsymbol{\Sigma}}_0$ in $\underline{\mathbf{c}}$ and from the condition $\underset{\approx}{\boldsymbol{\epsilon}} : \underset{\sim}{\boldsymbol{\Sigma}}_0 = \underline{\mathbf{c}}$ deduced from problem (29). Accordingly, the tensor of effective moduli possesses all symmetries of classical elastic moduli for a Cauchy medium:

$$A^{(1)}_{0\,ijkl} = A^{(1)}_{0\,klij} = A^{(1)}_{0\,jikl} = A^{(1)}_{0\,ijlk}.$$

The expression of the overall constitutive tensors reads

$$\underset{\approx}{\mathbf{A}}_0^{(1)} = \left\langle \underset{\approx}{\mathbf{a}}^{(0)} : \left(\underset{\approx}{\mathbf{1}} + \underline{\nabla}_y \otimes \underset{\sim}{\boldsymbol{X}}_u^{(1)} + \underset{\approx}{\boldsymbol{\epsilon}} \cdot \underset{\sim}{\boldsymbol{X}}_\phi^{(1)} \right) \right\rangle. \tag{35}$$

3.4. Second homogenization scheme

According to the HS2, the local constitutive equations are assumed to take the form:

$$\underset{\sim}{\boldsymbol{\sigma}}^{\varepsilon} = \underset{\approx}{\mathbf{a}}^{(0)}(\underline{\mathbf{y}}) : (\underline{\mathbf{u}}^{\varepsilon} \otimes \underline{\nabla} + \underset{\approx}{\boldsymbol{\epsilon}} \cdot \underline{\boldsymbol{\phi}}^{\varepsilon}), \qquad \underset{\sim}{\boldsymbol{\mu}}^{\varepsilon} = \underset{\approx}{\mathbf{c}}^{(2)}(\underline{\mathbf{y}}) : (\underline{\boldsymbol{\phi}}^{\varepsilon} \otimes \underline{\nabla}). \tag{36}$$

The different steps of the asymptotic analysis are the same as in Section 3.3 for HS1 and we will only focus here on the main results. In particular, $\underline{\mathbf{u}}_0$ and $\underline{\boldsymbol{\phi}}_1$ fulfill the following equations:

$$\underline{\mathbf{u}}_0 \otimes \underline{\nabla}_y = 0, \qquad \underline{\boldsymbol{\phi}}_1 \otimes \underline{\nabla}_y = 0, \tag{37}$$

the solutions of which are translations and constant micro-rotations on Y:

$$\underline{\mathbf{u}}_0(\underline{\mathbf{x}}, \underline{\mathbf{y}}) = \underline{\mathbf{U}}_0(\underline{\mathbf{x}}), \qquad \underline{\boldsymbol{\phi}}_1(\underline{\mathbf{x}}, \underline{\mathbf{y}}) = \underline{\boldsymbol{\Phi}}_1(\underline{\mathbf{x}}). \tag{38}$$

The terms $(\underline{\mathbf{u}}_1, \underline{\boldsymbol{\phi}}_2, \underset{\sim}{\boldsymbol{\sigma}}_0, \underset{\sim}{\boldsymbol{\mu}}_0)$ and $(\underline{\mathbf{u}}_2, \underline{\boldsymbol{\phi}}_3, \underset{\sim}{\boldsymbol{\sigma}}_1, \underset{\sim}{\boldsymbol{\mu}}_1)$ are then, respectively, solutions of the two following auxiliary problems on Y:

$$\begin{cases} \underset{\sim}{\mathbf{e}}_0 = (\underline{\mathbf{U}}_0 \otimes \underline{\nabla}_x + \underset{\approx}{\boldsymbol{\epsilon}} \cdot \underline{\boldsymbol{\Phi}}_1) + \underline{\mathbf{u}}_1 \otimes \underline{\nabla}_y, & \underset{\sim}{\boldsymbol{\kappa}}_0 = \underline{\boldsymbol{\Phi}}_1 \otimes \underline{\nabla}_x + \underline{\boldsymbol{\phi}}_2 \otimes \underline{\nabla}_y, \\ \underset{\sim}{\boldsymbol{\sigma}}_0 = \underset{\approx}{\mathbf{a}}^{(0)} : \underset{\sim}{\mathbf{e}}_0, & \underset{\sim}{\boldsymbol{\mu}}_0 = \underset{\approx}{\mathbf{c}}^{(2)} : \underset{\sim}{\boldsymbol{\kappa}}_0, \\ \underset{\sim}{\boldsymbol{\sigma}}_0 \cdot \underline{\nabla}_y = 0, & \underset{\sim}{\boldsymbol{\mu}}_0 \cdot \underline{\nabla}_y = 0, \end{cases} \tag{39}$$

$$\begin{cases} \underset{\sim}{\mathbf{e}}_1 = \underline{\mathbf{u}}_1 \otimes \underline{\nabla}_x + \underline{\mathbf{u}}_2 \otimes \underline{\nabla}_y + \underset{\approx}{\boldsymbol{\epsilon}} \cdot \underline{\boldsymbol{\phi}}_2, & \underset{\sim}{\boldsymbol{\kappa}}_1 = \underline{\boldsymbol{\phi}}_2 \otimes \underline{\nabla}_x + \underline{\boldsymbol{\phi}}_3 \otimes \underline{\nabla}_y, \\ \underset{\sim}{\boldsymbol{\sigma}}_1 = \underset{\approx}{\mathbf{a}}^{(0)} : \underset{\sim}{\mathbf{e}}_1, & \underset{\sim}{\boldsymbol{\mu}}_1 = \underset{\approx}{\mathbf{c}}^{(2)} : \underset{\sim}{\boldsymbol{\kappa}}_1, \\ \underset{\sim}{\boldsymbol{\sigma}}_0 \cdot \underline{\nabla}_x + \underset{\sim}{\boldsymbol{\sigma}}_1 \cdot \underline{\nabla}_y + \underline{\mathbf{f}} = 0, & \underset{\sim}{\boldsymbol{\mu}}_0 \cdot \underline{\nabla}_x + \underset{\sim}{\boldsymbol{\mu}}_1 \cdot \underline{\nabla}_y - \underset{\approx}{\boldsymbol{\epsilon}} : \underset{\sim}{\boldsymbol{\sigma}}_0 + \underline{\mathbf{c}} = 0. \end{cases} \tag{40}$$

The existence and uniqueness of a solution to problem (39) up to constant translations and micro-rotations is proved in Appendix B, whereas the problem (40) is treated by Pradel (1998). The problem (39) is linear in $\underset{\sim}{\mathbf{e}}_0$ and $\underline{\boldsymbol{\Phi}}_1 \otimes \underline{\nabla}_x$, so that the solution up to order ε^1 takes the form:

$$\underline{\mathbf{u}}^{\varepsilon} = \underline{\mathbf{U}}_0(\underline{\mathbf{x}}) + \varepsilon[\underline{\mathbf{U}}_1(\underline{\mathbf{x}}) + \underset{\approx}{\boldsymbol{X}}^{(2)}(\underline{\mathbf{y}}) : (\underline{\mathbf{U}}_0 \otimes \underline{\nabla}_x + \underset{\approx}{\boldsymbol{\epsilon}} \cdot \underline{\boldsymbol{\Phi}}_1)(\underline{\mathbf{x}})] \cdots, \tag{41}$$

$$\underline{\boldsymbol{\phi}}^{\varepsilon} = \underline{\boldsymbol{\Phi}}_1(\underline{\mathbf{x}}) + \varepsilon(\underline{\boldsymbol{\Phi}}_2(\underline{\mathbf{x}}) + \underset{\approx}{\boldsymbol{Z}}(\underline{\mathbf{y}}) : \underline{\boldsymbol{\Phi}}_1(\underline{\mathbf{x}}) \otimes \underline{\nabla}_x) + \cdots, \tag{42}$$

where concentration tensors $\underset{\approx}{\boldsymbol{X}}^{(2)}$ and $\underset{\approx}{\boldsymbol{Z}}$ have been introduced. They are such that their mean value over the unit cell vanishes. The fact that the problems in $\underline{\mathbf{u}}_1$ and $\underline{\boldsymbol{\phi}}_2$ in Eq. (39) are decoupled has been taken into account.

Main results of the analysis

The main results of the second analysis are given by Eqs. (43)–(46). The boundary value problem to be solved at the macroscopic level reads

$$\underset{\sim}{\boldsymbol{\Sigma}}_0 \cdot \underline{\nabla} + \underline{\mathbf{f}} = 0, \qquad \underset{\sim}{\mathbf{M}}_0 \cdot \underline{\nabla} - \underset{\approx}{\boldsymbol{\epsilon}} : \underset{\sim}{\boldsymbol{\Sigma}}_0 + \underline{\mathbf{c}} = 0, \tag{43}$$

$$\underset{\sim}{\boldsymbol{\Sigma}}_0 = \underset{\approx}{\mathbf{A}}_0^{(2)} : (\underline{\mathbf{U}}_0 \otimes \underline{\nabla} + \underset{\approx}{\boldsymbol{\epsilon}} \cdot \underline{\boldsymbol{\Phi}}_1), \qquad \underset{\sim}{\mathbf{M}}_0 = \underset{\approx}{\mathbf{C}}_0^{(2)} : (\underline{\boldsymbol{\Phi}}_1 \otimes \underline{\nabla}), \tag{44}$$

$$\underline{\mathbf{U}}_0 = 0, \qquad \underline{\boldsymbol{\Phi}}_1 = 0 \quad \text{on } \partial\Omega. \tag{45}$$

The effective medium is here a full Cosserat continuum. The effective constitutive tensors are related to the concentration tensors by

$$\begin{aligned} \underset{\approx}{\mathbf{A}}_0^{(2)} &= \left\langle \underset{\approx}{\mathbf{a}}^{(0)} : (\underset{\approx}{\mathbf{1}} + \underline{\nabla}_y \otimes \underset{\approx}{\boldsymbol{X}}^{(2)}) \right\rangle, \\ \underset{\approx}{\mathbf{C}}_0^{(2)} &= \left\langle \underset{\approx}{\mathbf{c}}^{(2)} : (\underset{\approx}{\mathbf{1}} + \underline{\nabla}_y \otimes \underset{\approx}{\boldsymbol{Z}}) \right\rangle. \end{aligned} \tag{46}$$

3.5. Formulation of the auxiliary problems on Y^l

For the applications, it is more convenient to work on the actual structure Ω than on the associated dimensionless body. That is why, it is useful to formulate the auxiliary problems on the actual unit cell Y^l. These auxiliary problems must be solved in order to compute the effective moduli. They will be solved in Section 5 using the finite-element method in the case of a specific micro-structure.

3.5.1. Homogenization scheme 1

We first define the sets of kinematically admissible strain fields and statically admissible stress fields exhibiting Y^l-periodicity:

$$\mathscr{KA}^{(1)} = \left\{ (\underset{\sim}{\mathbf{e}}, \underset{\sim}{\boldsymbol{\kappa}}) / \exists \underline{\mathbf{u}}^{\text{per}}, \underline{\boldsymbol{\phi}}^{\text{per}} \ Y^l\text{-periodic}, \qquad \left\{ \begin{array}{l} \underset{\sim}{\mathbf{e}} = \underline{\mathbf{u}}^{\text{per}} \otimes \underline{\nabla} + \underset{\approx}{\boldsymbol{\epsilon}} \cdot \underline{\boldsymbol{\phi}}^{\text{per}} \\ \underset{\sim}{\boldsymbol{\kappa}} = \underline{\boldsymbol{\phi}}^{\text{per}} \otimes \underline{\nabla} \end{array} \right\}, \right. \tag{47}$$

$$\mathscr{SA}^{(1)} = \left\{ (\underset{\sim}{\boldsymbol{\sigma}}, \underset{\sim}{\boldsymbol{\mu}}) / \underset{\sim}{\boldsymbol{\sigma}} \cdot \underline{\mathbf{n}}, \underset{\sim}{\boldsymbol{\mu}} \cdot \underline{\mathbf{n}} \text{ skew-periodic}, \qquad \left\{ \begin{array}{l} \underset{\sim}{\boldsymbol{\sigma}} \cdot \underline{\nabla} = 0 \\ \underset{\sim}{\boldsymbol{\mu}} \cdot \underline{\nabla} - \underset{\approx}{\boldsymbol{\epsilon}} : \underset{\sim}{\boldsymbol{\sigma}} = 0 \end{array} \right\}, \right. \tag{48}$$

where $\underline{\mathbf{n}}$ is the unit outer normal to the boundary of Y^l. The boundary value problem on Y^l deduced from Eq. (29) amounts then to finding out elements $(\underset{\sim}{\mathbf{e}}, \underset{\sim}{\boldsymbol{\kappa}}) \in \mathscr{KA}^{(1)}$ and $(\underset{\sim}{\boldsymbol{\sigma}}, \underset{\sim}{\boldsymbol{\mu}}) \in \mathscr{SA}^{(1)}$ related by the constitutive equations:

$$\underset{\sim}{\boldsymbol{\sigma}} = \underset{\approx}{\mathbf{a}}^l : (\underset{\sim}{\mathbf{e}} + \underset{\sim}{\mathbf{E}}^{\mathrm{s}}), \qquad \underset{\sim}{\boldsymbol{\mu}} = \underset{\approx}{\mathbf{c}}^l : \underset{\sim}{\boldsymbol{\kappa}} \tag{49}$$

for any given symmetric tensor $\underset{\sim}{\mathbf{E}}^{\mathrm{s}}$. The solutions then correspond to extrema of the mean potential and complementary energy:

$$\min_{(\underset{\sim}{\mathbf{e}}', \underset{\sim}{\boldsymbol{\kappa}}') \in \mathscr{KA}^{(1)}} \mathscr{W}(\underset{\sim}{\mathbf{e}}' + \underset{\sim}{\mathbf{E}}^{\mathrm{s}}, \underset{\sim}{\boldsymbol{\kappa}}') = \underset{\sim}{\mathbf{E}}^{s} : \underset{\approx}{\mathbf{A}}^{(1)} : \underset{\sim}{\mathbf{E}}^{\mathrm{s}} = \max_{(\underset{\sim}{\boldsymbol{\sigma}}', \underset{\sim}{\boldsymbol{\mu}}') \in \mathscr{SA}^{(1)}} (2\langle \underset{\sim}{\boldsymbol{\sigma}}' \rangle_{Y^l} : \underset{\sim}{\mathbf{E}}^{\mathrm{s}} - \mathscr{W}^*(\underset{\sim}{\boldsymbol{\sigma}}', \underset{\sim}{\boldsymbol{\mu}}')) \tag{50}$$

with

$$\mathscr{W}(\underset{\sim}{\mathbf{e}}, \underset{\sim}{\boldsymbol{\kappa}}) = \left\langle \underset{\sim}{\mathbf{e}}^{\mathrm{T}} : \underset{\approx}{\mathbf{a}}^l : \underset{\sim}{\mathbf{e}} + \underset{\sim}{\boldsymbol{\kappa}} : \underset{\approx}{\mathbf{c}}^l : \underset{\sim}{\boldsymbol{\kappa}} \right\rangle_{Y^l}, \tag{51}$$

$$\mathscr{W}^*(\underset{\sim}{\boldsymbol{\sigma}}, \underset{\sim}{\boldsymbol{\mu}}) = \left\langle \underset{\sim}{\boldsymbol{\sigma}} : \underset{\approx}{\mathbf{a}}^{l-1} : \underset{\sim}{\boldsymbol{\sigma}} + \underset{\sim}{\boldsymbol{\mu}} : \underset{\approx}{\mathbf{c}}^{l-1} : \underset{\sim}{\boldsymbol{\mu}} \right\rangle_{Y^l}. \tag{52}$$

As for them, the effective moduli are defined by

$$\underset{\approx}{\mathbf{A}}^{(1)} = \left\langle \underset{\approx}{\mathbf{a}}^l : (\underset{\approx}{\mathbf{1}} + \underset{\sim}{\boldsymbol{\nabla}} \otimes l\underset{\approx}{\boldsymbol{X}}_u^{(1)} + \underset{\approx}{\boldsymbol{\epsilon}} \cdot \underset{\approx}{\boldsymbol{X}}_{\phi}^{(1)}) \right\rangle_{Y^l}. \tag{53}$$

The concentration tensors involved in this expression are obtained by solving the previous boundary value problem successively for six loading conditions $\underset{\sim}{\mathbf{E}}^{\mathrm{s}(ij)}$ defined by the Cartesian components $E_{kl}^{\mathrm{s}(ij)} = (1/2)(\delta_{ik}\delta_{jl} + \delta_{il}\delta_{jk})$. The effective elastic moduli fulfill the major and minor symmetry conditions:

$$A_{ijkl}^{(1)} = A_{klij}^{(1)} = A_{jikl}^{(1)} = A_{ijlk}^{(1)}.$$

3.5.2. Homogenization scheme 2

In this case, the sets of kinematically admissible strain fields and statically admissible stress fields exhibiting Y^l-periodicity are defined as follows:

$$\mathscr{KA}_u^{(2)} = \left\{ \underset{\sim}{\mathbf{e}} / \exists \underline{\mathbf{u}}^{\mathrm{per}} \ Y^l\text{-periodic} / \underset{\sim}{\mathbf{e}} = \underline{\mathbf{u}}^{\mathrm{per}} \otimes \underline{\boldsymbol{\nabla}} \right\}, \tag{54}$$

$$\mathscr{KA}_{\phi}^{(2)} = \left\{ \underset{\sim}{\boldsymbol{\kappa}} / \exists \underline{\boldsymbol{\phi}}^{\mathrm{per}} \ Y^l\text{-periodic} / \underset{\sim}{\boldsymbol{\kappa}} = \underline{\boldsymbol{\phi}}^{\mathrm{per}} \otimes \underline{\boldsymbol{\nabla}} \right\}, \tag{55}$$

$$\mathscr{SA}_{\sigma}^{(2)} = \left\{ \underset{\sim}{\boldsymbol{\sigma}} / \underset{\sim}{\boldsymbol{\sigma}} \cdot \underline{\mathbf{n}} \text{ skew-periodic}, \underset{\sim}{\boldsymbol{\sigma}} \cdot \underline{\boldsymbol{\nabla}} = 0 \right\}, \tag{56}$$

$$\mathscr{SA}_{\mu}^{(2)} = \left\{ \underset{\sim}{\boldsymbol{\mu}} / \underset{\sim}{\boldsymbol{\mu}} \cdot \underline{\mathbf{n}} \text{ skew-periodic}, \underset{\sim}{\boldsymbol{\mu}} \cdot \underline{\boldsymbol{\nabla}} = 0 \right\}. \tag{57}$$

Two boundary value problems on Y^l can be deduced from Eq. (39). For, the problems in force stresses and couple stresses can be decoupled. It amounts then to finding out an element $(\underset{\sim}{\mathbf{e}}, \underset{\sim}{\boldsymbol{\kappa}})$ of the Cartesian product $\mathscr{KA}^{(2)} = \mathscr{KA}_u^{(2)} \times \mathscr{KA}_{\phi}^{(2)}$ and $(\underset{\sim}{\boldsymbol{\sigma}}, \underset{\sim}{\boldsymbol{\mu}}) \in \mathscr{SA}^{(2)} = \mathscr{SA}_{\sigma}^{(2)} \times \mathscr{SA}_{\mu}^{(2)}$ related by the constitutive equations:

$$\underset{\sim}{\boldsymbol{\sigma}} = \underset{\approx}{\mathbf{a}}^l : (\underset{\sim}{\mathbf{e}} + \underset{\sim}{\mathbf{E}}), \qquad \underset{\sim}{\boldsymbol{\mu}} = \underset{\approx}{\mathbf{c}}^l : (\underset{\sim}{\boldsymbol{\kappa}} + \underset{\sim}{\mathbf{K}}) \tag{58}$$

for any given second-rank tensors $\underset{\sim}{\mathbf{E}}$ and $\underset{\sim}{\mathbf{K}}$. The solutions then correspond to extrema of the mean potential or complementary energy:

$$\min_{\underset{\sim}{\mathbf{e}}' \in \mathscr{K}\mathscr{A}_{\mathbf{u}}^{(2)}} \mathscr{W}_u(\underset{\sim}{\mathbf{e}}' + \underset{\sim}{\mathbf{E}}) = \underset{\sim}{\mathbf{E}} : \underset{\approx}{\mathbf{A}}^{(2)} : \underset{\sim}{\mathbf{E}} = \max_{\underset{\sim}{\boldsymbol{\sigma}}' \in \mathscr{S}\mathscr{A}_{\sigma}^{(2)}} (2\langle \underset{\sim}{\boldsymbol{\sigma}}' \rangle : \underset{\sim}{\mathbf{E}} - \mathscr{W}_{\sigma}^{*}(\underset{\sim}{\boldsymbol{\sigma}}')), \tag{59}$$

$$\min_{\underset{\sim}{\boldsymbol{\kappa}}' \in \mathscr{K}\mathscr{A}_{\phi}^{(2)}} \mathscr{W}_{\phi}(\underset{\sim}{\boldsymbol{\kappa}}' + \underset{\sim}{\mathbf{K}}) = \underset{\sim}{\mathbf{K}} : \underset{\approx}{\mathbf{C}}^{(2)} : \underset{\sim}{\mathbf{K}} = \max_{\underset{\sim}{\boldsymbol{\mu}}' \in \mathscr{S}\mathscr{A}_{\mu}^{(2)}} (2\langle \underset{\sim}{\boldsymbol{\mu}}' \rangle : \underset{\sim}{\mathbf{K}} - \mathscr{W}_{\mu}^{*}(\underset{\sim}{\boldsymbol{\mu}}')) \tag{60}$$

with

$$\mathscr{W}_u(\underset{\sim}{\mathbf{e}}) = \langle \underset{\sim}{\mathbf{e}} : \underset{\approx}{\mathbf{a}}^{l} : \underset{\sim}{\mathbf{e}} \rangle_{Y^l}, \qquad \mathscr{W}_{\phi}(\underset{\sim}{\boldsymbol{\kappa}}) = \langle \underset{\sim}{\boldsymbol{\kappa}} : \underset{\approx}{\mathbf{c}}^{l} : \underset{\sim}{\boldsymbol{\kappa}} \rangle_{Y^l}, \tag{61}$$

$$\mathscr{W}_{\sigma}^{*}(\underset{\sim}{\boldsymbol{\sigma}}) = \langle \underset{\sim}{\boldsymbol{\sigma}} : \underset{\approx}{\mathbf{a}}^{l-1} : \underset{\sim}{\boldsymbol{\sigma}} \rangle_{Y^l} \qquad \mathscr{W}_{\mu}^{*}(\underset{\sim}{\boldsymbol{\mu}}) = \langle \underset{\sim}{\boldsymbol{\mu}} : \underset{\approx}{\mathbf{c}}^{l-1} : \underset{\sim}{\boldsymbol{\mu}} \rangle_{Y^l}. \tag{62}$$

As for them, the effective moduli are defined by

$$\underset{\approx}{\mathbf{A}}^{(2)} = \left\langle \underset{\approx}{\mathbf{a}}^{l} : (\underset{\approx}{\mathbf{1}} + \underline{\nabla} \otimes l\underset{\approx}{\boldsymbol{X}}^{(2)}) \right\rangle_{Y^l}, \qquad \underset{\approx}{\mathbf{C}}^{(2)} = \left\langle \underset{\approx}{\mathbf{c}}^{l} : (\underset{\approx}{\mathbf{1}} + \underline{\nabla} \otimes l\underset{\approx}{\boldsymbol{Z}}) \right\rangle_{Y^l}. \tag{63}$$

The concentration tensors involved in these expressions are obtained by solving the previous boundary value problems successively for 18 loading conditions $\underset{\sim}{\mathbf{E}}^{(ij)}$ and $\underset{\sim}{\mathbf{K}}^{(ij)}$ defined by their Cartesian components $E_{kl}^{(ij)} = K_{kl}^{(ij)} = \delta_{ik}\delta_{jl}$. The effective elasticity tensors display the major symmetry properties:

$$A_{ijkl}^{(2)} = A_{klij}^{(2)}, \qquad C_{ijkl} = C_{klij}.$$

3.6. Links between HS1 and HS2

Some relationships between the effective properties $\underset{\approx}{\mathbf{A}}^{(i)}$ and $\underset{\approx}{\mathbf{C}}^{(i)}$ $(i = 1, 2)$ can be established using the variational formulation of each homogenization scheme.

The elasticity tensors $\underset{\approx}{\mathbf{A}}^{(1)}$ and $\underset{\approx}{\mathbf{A}}^{(2)}$ cannot be directly compared since the first one operates on symmetric second-rank tensors, whereas the second one operates on general second-rank tensors. However, $\underset{\approx}{\mathbf{A}}^{(1)}$ can be compared to a "Cauchy part" of $\underset{\approx}{\mathbf{A}}^{(2)}$ that can be defined as follows:

$$\underset{\sim}{\mathbf{E}}^{\mathrm{s}} : \underset{\approx}{\mathbf{A}}^{(2s)} : \underset{\sim}{\mathbf{E}}^{\mathrm{s}} = \min_{\{\underline{\boldsymbol{\Omega}}' / \underset{\sim}{\mathbf{E}} = \underset{\sim}{\mathbf{E}}^{s} + \underset{\simeq}{\boldsymbol{\epsilon}} \cdot \underline{\boldsymbol{\Omega}}\}} \underset{\sim}{\mathbf{E}} : \underset{\approx}{\mathbf{A}}^{(2)} : \underset{\sim}{\mathbf{E}}, \quad \forall \underset{\sim}{\mathbf{E}}^{\mathrm{s}} \text{symmetric}. \tag{64}$$

Then, the following properties hold:

$$\underset{\approx}{\mathbf{A}}^{(1)} \leqslant \underset{\approx}{\mathbf{A}}^{(2\mathrm{s})}, \qquad \lim_{l_{\mathrm{c}} \to \infty} \underset{\approx}{\mathbf{A}}^{(1)} = \underset{\approx}{\mathbf{A}}^{(2\mathrm{s})}. \tag{65}$$

The previous inequality holds in the sense of quadratic forms operating on symmetric second-rank tensors. This result stems from the fact that an element of $\mathscr{K}\mathscr{A}_{u}^{(2)}$ and constant micro-rotations $\underline{\boldsymbol{\phi}}^{\mathrm{per}}$ are in $\mathscr{K}\mathscr{A}^{(1)}$ and can therefore be used in the variational formulation (50). The proof of the second result is more subtle: consider the field $\underset{\sim}{\boldsymbol{\sigma}}^{2}$ solution of HS2 for a given $\underset{\sim}{\mathbf{E}}^{\mathrm{s}}$ and the associated macro-rotation $\underline{\boldsymbol{\Omega}}$ realizing the minimum of Eq. (64). The associated macro-stress is symmetric i.e. $\langle \underset{\simeq}{\boldsymbol{\epsilon}} : \underset{\sim}{\boldsymbol{\sigma}}^{2} \rangle = 0$. There exists therefore a periodic couple-stress field $\underset{\sim}{\boldsymbol{\mu}}'$ such that $\underset{\sim}{\boldsymbol{\mu}}' \cdot \underline{\nabla} - \underset{\simeq}{\boldsymbol{\epsilon}} : \underset{\sim}{\boldsymbol{\sigma}}^{2} = 0$. The pair $(\underset{\sim}{\boldsymbol{\sigma}}^{2}, \underset{\sim}{\boldsymbol{\mu}}')$ is an element of $\mathscr{S}\mathscr{A}^{(1)}$ and can be used in the variational formulation (50). Then, let l_{c} go to infinity (i.e. the norm of $\underset{\approx}{\mathbf{c}}^{l-1}$ go to zero) and the result follows.

4. An intermediate homogenization scheme

A heuristic homogenization scheme, labelled HS3 in the sequel, is proposed here that is not deduced from the previous asymptotic analyses but rather combines features of both schemes HS1 and HS2. The two investigated schemes represent in fact two extreme cases. In the first case, the constitutive equations for deformation and curvature are coupled at the local level via the micro-rotation $\underset{\sim}{\boldsymbol{\phi}}$ (see Eq. (47)) but the resulting effective continuum is a Cauchy medium. In contrast, in the second case, the problems in displacement and micro-rotation are fully decoupled (see Eqs. (54) and (55)). It is known that, in the case of a non-linear local behavior, the influence of local micro-rotation on the stress response can play a major role (in the case of polycrystals for instance see Smyshlyaev and Fleck (1996) and Forest et al. (2000)). In the non-linear case, the secant or tangent Cosserat stiffness associated with l_c may vary during the deformation process. It may become stiffer or undergo some softening, so that l_c may lie in the unshaded zone of Fig. 1. An intermediate scheme resorting to coupled strain measures like $\mathscr{KA}^{(1)}$ and allowing to prescribe a mean curvature and therefore leading to a Cosserat effective medium, may be useful for a heuristic extension to non-linear behaviors. Although this third scheme cannot be derived in a rigorous manner like HS1 and HS2 and although other variants may exist, it is possible to propose a sound framework by introducing the following sets of admissible fields:

$$\mathscr{KA}^{(3)} = \left\{ (\underset{\sim}{\mathbf{e}}, \underset{\sim}{\boldsymbol{\kappa}}) \in \mathscr{KA}^{(1)} \quad \langle \underset{\sim}{\mathbf{e}} \rangle = 0 \right\}, \tag{66}$$

$$\mathscr{SA}^{(3)} = \left\{ (\underset{\sim}{\boldsymbol{\sigma}}, \underset{\sim}{\boldsymbol{\mu}}) / \underset{\sim}{\boldsymbol{\sigma}} \cdot \underline{\mathbf{n}}, \underset{\sim}{\boldsymbol{\mu}} \cdot \underline{\mathbf{n}} \text{ skew-periodic}, \qquad \left\{ \begin{array}{l} \underset{\sim}{\boldsymbol{\sigma}} \cdot \underline{\mathbf{V}} = 0 \\ \underset{\sim}{\boldsymbol{\mu}} \cdot \underline{\mathbf{V}} - \underset{\simeq}{\boldsymbol{\epsilon}} : \underset{\sim}{\boldsymbol{\sigma}} = \text{constant} \end{array} \right. \right\}. \tag{67}$$

The proposed boundary value problem on the unit cell amounts to finding out $(\underset{\sim}{\mathbf{e}}, \underset{\sim}{\boldsymbol{\kappa}}) \in \mathscr{KA}^{(3)}$ and $(\underset{\sim}{\boldsymbol{\sigma}}, \underset{\sim}{\boldsymbol{\mu}}) \in \mathscr{SA}^{(3)}$ related by the constitutive relations:

$$\underset{\sim}{\boldsymbol{\sigma}} = \underset{\approx}{\mathbf{a}}^{l} : (\underset{\sim}{\mathbf{E}} + \underset{\sim}{\mathbf{e}}), \qquad \underset{\sim}{\boldsymbol{\mu}} = \underset{\approx}{\mathbf{c}}^{l} : (\underset{\sim}{\mathbf{K}} + \underset{\sim}{\boldsymbol{\kappa}}) \tag{68}$$

for given tensors $\underset{\sim}{\mathbf{E}}$ and $\underset{\sim}{\mathbf{K}}$. The introduction of the additional condition $\langle \underset{\sim}{\mathbf{e}} \rangle_{Y^l} = 0$ (which is equivalent to $\langle \underset{\sim}{\boldsymbol{\phi}}^{\text{per}} \rangle = 0$) and of a constant in the last balance equation in $\mathscr{SA}^{(3)}$ gives the possibility of prescribing a relative rotation to the unit cell, which was not possible using HS1. The solutions correspond to extrema of the potential and complementary energy:

$$\begin{aligned} \underset{\sim}{\mathbf{E}} : \underset{\approx}{\mathbf{A}}^{(3)} : \underset{\sim}{\mathbf{E}} + \underset{\sim}{\mathbf{K}} : \underset{\approx}{\mathbf{C}}^{(3)} : \underset{\sim}{\mathbf{K}} &= \min_{(\underset{\sim}{\mathbf{e}}', \underset{\sim}{\boldsymbol{\kappa}}') \in \mathscr{KA}^{(3)}} \mathscr{W}(\underset{\sim}{\mathbf{e}}' + \underset{\sim}{\mathbf{E}}, \underset{\sim}{\boldsymbol{\kappa}}' + \underset{\sim}{\mathbf{K}}) \\ &= \max_{(\underset{\sim}{\boldsymbol{\sigma}}', \underset{\sim}{\boldsymbol{\mu}}') \in \mathscr{SA}^{(3)}} (2\underset{\sim}{\mathbf{E}} : \langle \underset{\sim}{\boldsymbol{\sigma}}' \rangle_{Y^l} + 2\underset{\sim}{\mathbf{K}} : \langle \underset{\sim}{\boldsymbol{\mu}}' \rangle_{Y^l} - \mathscr{W}^*(\underset{\sim}{\boldsymbol{\sigma}}', \underset{\sim}{\boldsymbol{\mu}}')), \end{aligned} \tag{69}$$

where $\mathscr{W}$ and $\mathscr{W}^*$ are given by Eqs. (51) and (52).

The effective elasticity tensors $\underset{\approx}{\mathbf{A}}^{(3)}$ and $\underset{\approx}{\mathbf{C}}^{(3)}$ are determined by solving the previous boundary value problem on the unit cell for 18 loading conditions $\underset{\sim}{\mathbf{E}}$ and $\underset{\sim}{\mathbf{K}}$. A coupling term between $\underset{\sim}{\mathbf{E}}$ and $\underset{\sim}{\mathbf{K}}$ may in general arise in the effective behavior (69) but, if the unit cell admits a symmetry point, it can be shown to vanish.

4.1. Links with the previous schemes

As in Section 3.6, a "Cauchy part" $\underset{\approx}{\mathbf{A}}^{(3s)}$ of $\underset{\approx}{\mathbf{A}}^{(3)}$ can be defined according to Eq. (64). Then, it can be seen that

$$\underset{\approx}{\mathbf{A}}^{(3s)} = \underset{\approx}{\mathbf{A}}^{(1)}. \tag{70}$$

It means that the third homogenization scheme has been constructed such that it gives the same "classical" moduli as HS1.

On the other hand, the following inequalities and limit relations hold:

$$\underset{\approx}{\mathbf{A}}^{(3)} \leqslant \underset{\approx}{\mathbf{A}}^{(2)}, \qquad \underset{\approx}{\mathbf{C}}^{(2)} \leqslant \underset{\approx}{\mathbf{C}}^{(3)}, \tag{71}$$

$$\lim_{l_c\to\infty} \underset{\approx}{\mathbf{A}}^{(3)} = \underset{\approx}{\mathbf{A}}^{(2)} \qquad \forall \underset{\sim}{\mathbf{K}} \neq 0 \quad \lim_{l_c\to\infty} \frac{\underset{\sim}{\mathbf{K}} : \underset{\approx}{\mathbf{C}}^{(3)} : \underset{\sim}{\mathbf{K}}}{\underset{\sim}{\mathbf{K}} : \underset{\approx}{\mathbf{C}}^{(2)} : \underset{\sim}{\mathbf{K}}} = 1. \tag{72}$$

The inequalities hold in the sense of quadratic forms on general second rank tensors. The inequality involving the bending stiffness $\underset{\approx}{\mathbf{C}}^{(3)}$ is valid only in the case of a centrosymmetric unit cell for which there is no additional effective tensor coupling macro-deformation and curvature. The previous results are direct applications of the variational formulations (59), (60) and (69) for well-suited trial fields.

5. Application to fiber matrix composites

5.1. Determination of the effective properties according to three homogenization schemes

We consider an Aluminum–SiC metal matrix composite in the linear range of mechanical response. For simplicity, the material is assumed to have a periodic microstructure and a square distribution of cylindrical fibers is considered. Two SiC volume fractions are studied: $f = 40\%$ and 10%. The unit cell is the square of Fig. 3(a) for $f = 40\%$, with a size of the square $l = 1$ mm. The elastic properties of the fiber are classical and read

$$E = 450 \text{ GPa}, \quad \nu = 0.25.$$

The aluminum matrix is taken as an isotropic linear elastic Cosserat medium (see Zhu et al. (1997) for the case of a strain-gradient matrix). The isotropic constitutive equations read

$$\underset{\sim}{\boldsymbol{\sigma}} = \lambda \underset{\sim}{\mathbf{1}} \operatorname{Tr} \underset{\sim}{\mathbf{e}} + 2\mu \, \{\underset{\sim}{\mathbf{e}}\} + 2\mu_c \, \}\underset{\sim}{\mathbf{e}}\{ \quad \text{and} \quad \underset{\sim}{\boldsymbol{\mu}} = \alpha \underset{\sim}{\mathbf{1}} \operatorname{Tr} \underset{\sim}{\boldsymbol{\kappa}} + 2\beta \, \{\underset{\sim}{\boldsymbol{\kappa}}\} + 2\gamma \, \}\underset{\sim}{\boldsymbol{\kappa}}\{, \tag{73}$$

where six elastic constants are involved (the (resp. inverted) braces denote the (resp. skew) symmetric part). In the two-dimensional case, α does not intervene and one usually takes $\beta = \gamma$ (de Borst, 1991). A characteristic length can then be defined:

$$l_c = \sqrt{\beta/\mu}. \tag{74}$$

In the computation, the SiC constituent is treated as a Cosserat medium with a insignificant small characteristic length. The classical moduli for aluminum read $E = 70$ GPa, $\nu = 0.3$. In the following, the parameter μ_c is fixed to 100 GPa, whereas several characteristic lengths l_c ranging from 10^{-4} to 10^2 mm will be considered. An equivalent analysis could be the study of a wide range of fiber diameters for a fixed l_c. The wanted effective properties exhibit cubic symmetry (Ilcewicz et al., 1986) and the considered overall elastic constants are written in the following form in the two-dimensional case:

$$\begin{bmatrix} \Sigma_{11} \\ \Sigma_{22} \\ \Sigma_{12} \\ \Sigma_{21} \\ M_{31} \\ M_{32} \end{bmatrix} = \begin{bmatrix} D_{1111} & D_{1122} & 0 & 0 & 0 & 0 \\ D_{1122} & D_{1111} & 0 & 0 & 0 & 0 \\ 0 & 0 & D_{1212} & D_{1221} & 0 & 0 \\ 0 & 0 & D_{1221} & D_{1212} & 0 & 0 \\ 0 & 0 & 0 & 0 & C^{\mathrm{h}}_{3131} & 0 \\ 0 & 0 & 0 & 0 & 0 & C^{\mathrm{h}}_{3131} \end{bmatrix} \begin{bmatrix} E_{11} \\ E_{22} \\ E_{12} \\ E_{21} \\ K_{31} \\ K_{32} \end{bmatrix} \tag{75}$$

for a general Cosserat effective medium. In the following, we will use the parameters,

$$\beta^{\mathrm{h}} = C^{\mathrm{h}}_{3131}/2, \quad \mu^{\mathrm{h}}_{\mathrm{c}} = (D_{1212} - D_{1221})/2.$$

The effective properties are determined using the finite-element method under plane strain conditions.

5.1.1. Homogenization scheme 1

A weak formulation of the boundary value problem defined by Eqs. (47)–(49) has been implemented in the finite-element program ZéBuLoN (Besson and Foerch, 1997). According to the first homogenization scheme (Section 3.3), the effective medium is a Cauchy continuum for which the classical cubic elastic constants can be determined for the two considered volume fractions: $D_{1212} = D_{1221}$, the relevant shear strain measure being $(E_{12} - E_{21})/2$, and C_{3131} does not exist in this case. The obtained effective moduli are given in Table 2 for $l_{\mathrm{c}}/l = 1$. The dependence of the effective moduli on the intrinsic length of the matrix is shown in Fig. 2. These dependence is rather slight for D_{1111} and D_{1122} and more pronounced for the effective shear modulus.

5.1.2. Homogenization scheme 2

The second homogenization scheme leads to a Cosserat effective medium for which the overall constants are now determined, using a finite-element formulation of Eqs. (54)–(58). The problems in $\underline{\mathbf{u}}^{\mathrm{per}}$ and in $\underline{\boldsymbol{\phi}}^{\mathrm{per}}$ are in fact decoupled, so that the effective constants D_{ijkl} do not depend on the characteristic length l_{c} as defined by Eq. (74). They do depend however on parameter μ_{c} and are given in Table 3. A linear relationship is found between β^{h} and β in the matrix for a fixed value of μ_{c}: $\beta^{\mathrm{h}} = 0.442\beta$ for $f = 40\%$ and $\beta^{\mathrm{h}} = 0.815\beta$ for $f = 10\%$. Note that for $f = 0$, the chosen Cosserat elastic constants of the aluminum matrix are retrieved. The deformed state of the unit cell after prescribing a symmetric (resp. skew-symmetric) overall Cosserat deformation $\underset{\sim}{\mathbf{E}}$ is shown on Fig. 3(b) (resp. 4(a)).

5.1.3. Homogenization scheme 3

A third heuristic homogenization scheme has been proposed in Section 4 that combines some features of HS1 and HS2. The effective medium is again a Cosserat continuum. The main advantage of this approach in comparison to HS2 is that the problems in displacements and micro-rotations are now coupled. This approach may be relevant in the case of a non-linear local behavior for which the asymptotic method may become untractable. The additional condition that the mean value of micro-rotation vanishes Eq. (66) is implemented using a penalty method. The found moduli D_{1111} and D_{1122} are identical to those obtained using HS1. The moduli D_{1212} and D_{1221} are found to be identical for HS2 and HS3. The application of a mean curvature on the unit cell is shown on Fig. 4(b). The dependence of the ratio of effective bending

Table 2
Effective properties of the Al–SiC fiber matrix composite according to HS1 (for $l_{\mathrm{c}}/l = 1$)

f	D_{1111} (MPa)	D_{1122} (MPa)	D_{1212} (MPa)
40%	163316	49060	57663
10%	108778	41560	33660

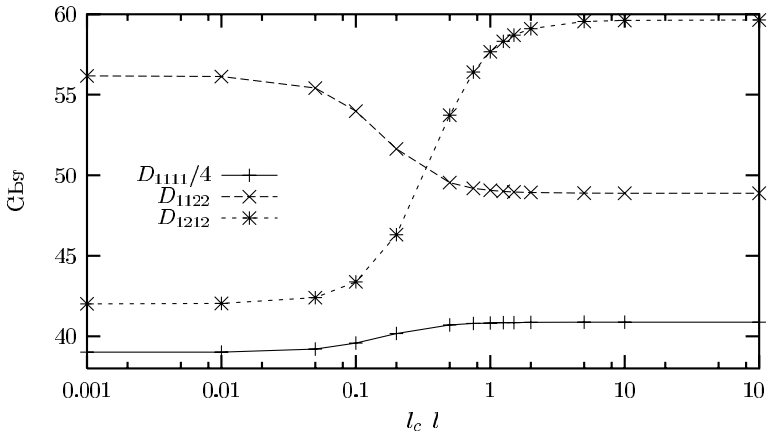

Fig. 2. Dependence of the effective moduli D_{ijkl} on the intrinsic length l_c of the matrix according to HS1 (for $f = 40\%$).

Table 3
Effective properties of the Al–SiC fiber matrix composite according to HS2

f	D_{1111} (MPa)	D_{1122} (MPa)	D_{1212} (MPa)	D_{1221} (MPa)
40%	163493	48884	85351	33927
10%	108863	41474	99055	−31307

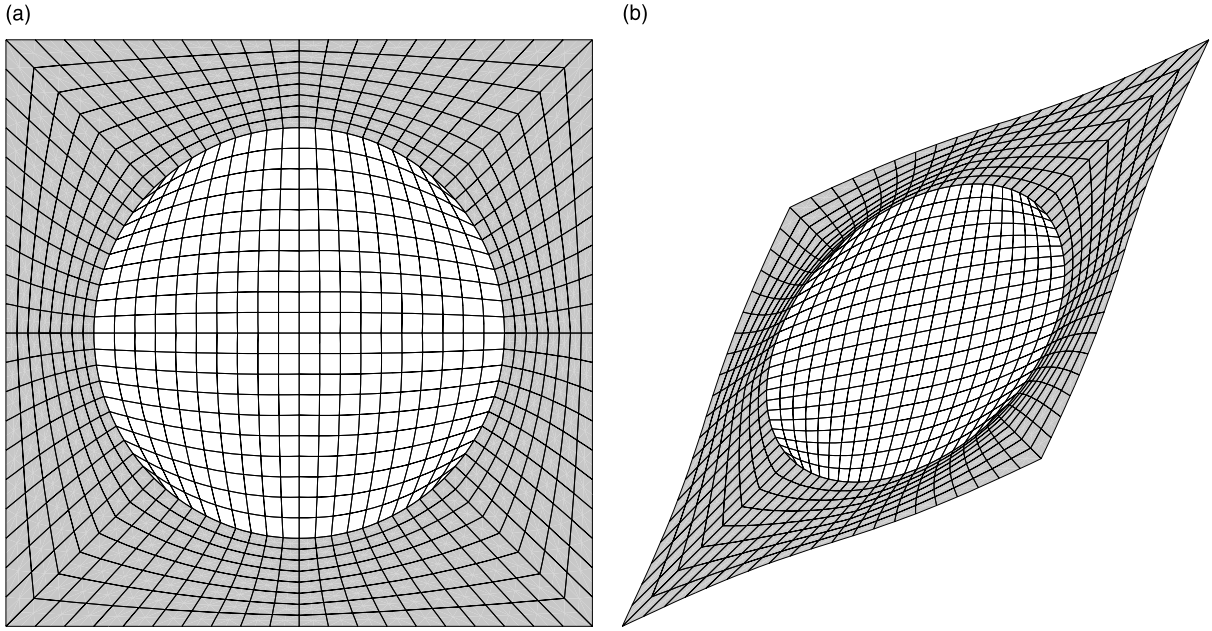

Fig. 3. Unit cell for a fiber matrix composite with $f = 40\%$ (left (a)); prescribed simple shear on the unit cell according to HS1 ($l_c/l = 1$, $E_{12} = E_{21} = 0.5$, right (b)).

stiffnesses $\beta^{h(3)}/\beta^{h(2)}$ on l_c is given in Fig. 5. $\beta^{h(3)}$ is not a linear function of β, contrary to the result of HS2. For large l_c the solution tends to that of HS2, as expected from the second term of relation (72). These results are in accordance with the predicted links between HS3 and the other schemes.

5.2. Application to structural calculations

The quality of the found effective medium can be assessed using structural calculations. On the one hand, a structure made of a finite number of fiber matrix cells is subjected to specific boundary conditions. For this first computation, every heterogenity is taken into account. It results in a very fine mesh and the resolution can be very time-consuming. The actual behavior of the two phases is explicitly used. That is why this computation is referred to as the reference one. On the other hand, the same structure under the same loading conditions is considered using homogeneous material properties, namely that of the effective medium resulting from the previous homogenization procedures. The prediction of this more simple calculation can then be compared with the results of the reference one. Similar structural calculations have been provided in (Forest and Sab, 1998) for HS2. This methodology is applied here to fiber metal matrix composites and the different homogenization schemes are compared for two types of loading conditions.

5.2.1. Cosserat glide test

We consider a square plate made of 5×5 cells. At the bottom of the structure, displacements U_1 and U_2 and micro-rotation Φ_3 are set to 0. At the top, a micro-rotation $\Phi_3 = 1$ is prescribed, whereas displacements are left free (Fig. 6(a)). The same loading conditions are applied to a square plate having the same

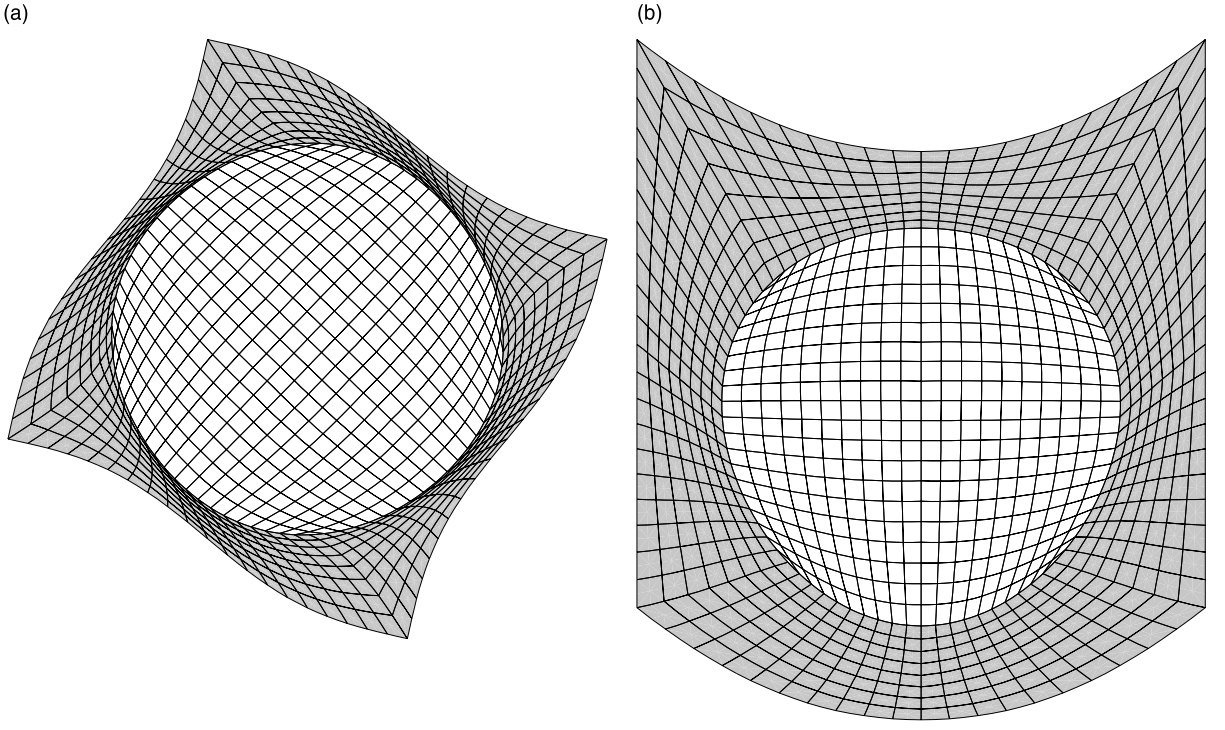

Fig. 4. Relative rotation prescribed on the unit cell according to HS2 ($E_{12} = -E_{21} = 0.5$, left (a)); mean curvature $K_{31} = 1$ on the unit cell according to HS3 (right (b)).

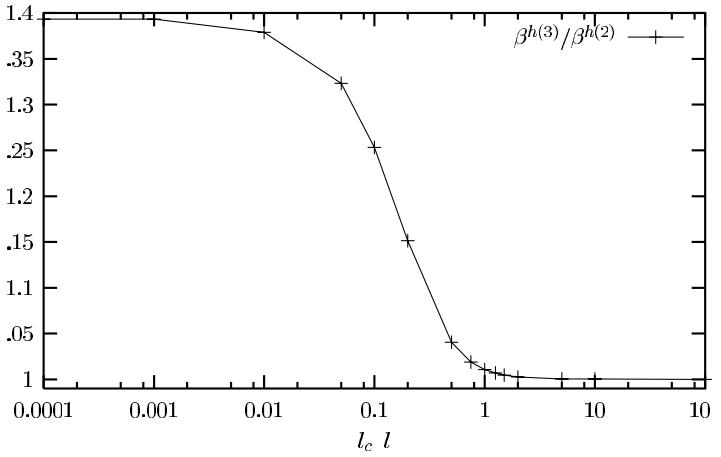

Fig. 5. Dependence of the ratio $\beta^{h(3)}/\beta^{h(2)}$ on the intrinsic length l_c of the matrix according to HS3 and HS2 (for $f = 40\%$).

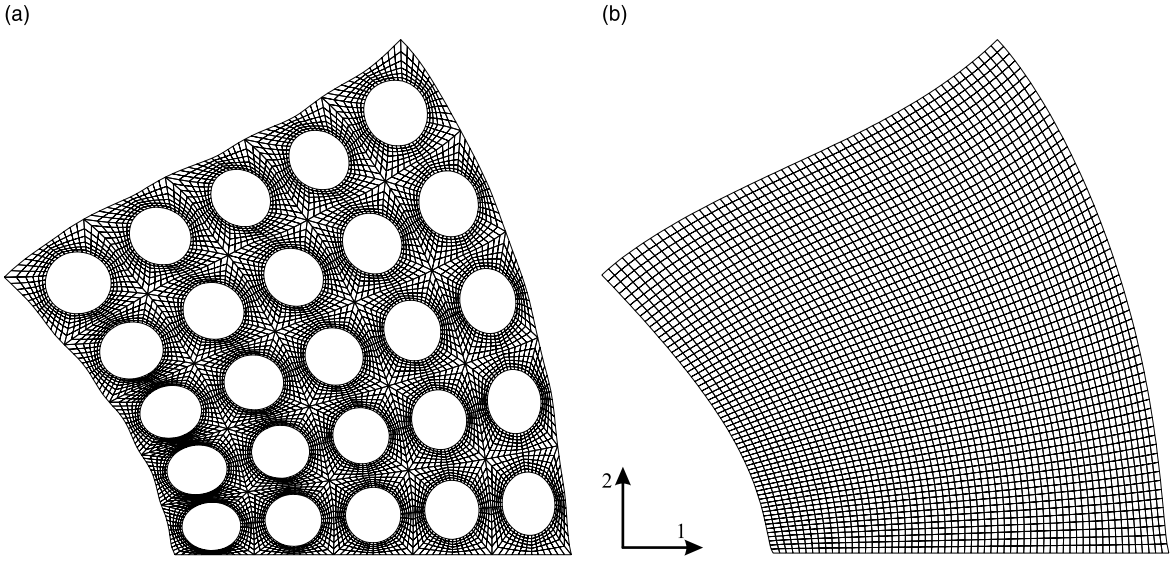

Fig. 6. Cosserat glide test on (a) a fiber matrix composite with $l_c/l = 5$ (left, the mesh of the fibers has not been represented) and (b) on the homogeneous equivalent medium according to HS2 (right).

dimensions and endowed with the effective properties according to HS1, HS2 or HS3. It must be noted that under this loading conditions, the use of the effective Cauchy medium HS1 leads to vanishing displacements and stresses, which corresponds to the classical solution of this problem. In contrast, the deformed state of the structure made of the full Cosserat effective medium HS2 is shown on Fig. 6(b). The response of this medium is compared with the reference one successively for $l_c = 5$ and 0.1 mm (Fig. 7). The comparison is drawn for the displacements and micro-rotations along a vertical line crossing the 5 inclusions of the fourth row from the left (Fig. 7). It appears that homogenization scheme, HS2 provides the best description of the structure when l_c/l is large. This is in agreement with the hypotheses of the asymptotic analysis. For smaller l_c, the HS2 prediction is less satisfactory (Fig. 7(b)).

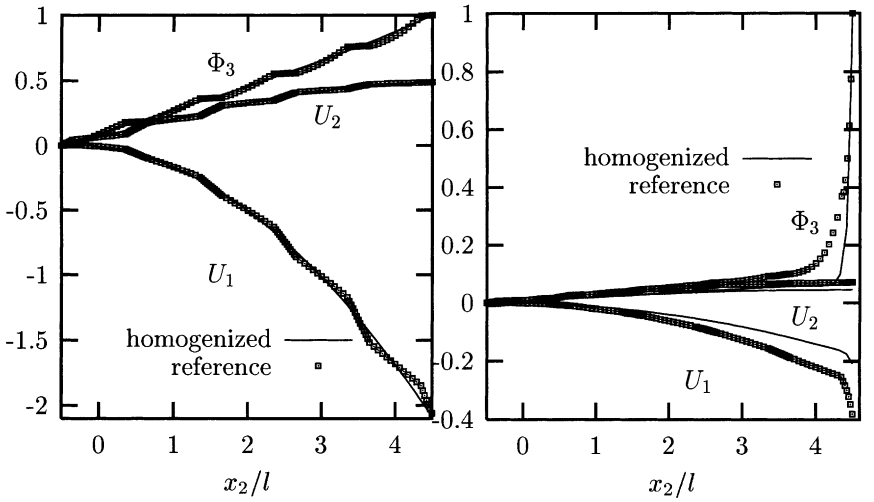

Fig. 7. Comparison of the displacements and micro-rotation along a vertical line in the middle of the fourth row, given by the reference calculation and the homogeneous equivalent medium according to HS2: Φ_3, U_2/l, U_1/l from the top to the bottom; (a) $l_c/l = 5$ (left), (b) $l_c/l = 0.1$ (right).

5.2.2. Combined shear and flexion test

Like in the previous test, the bottom of the structure is fixed in displacement and micro-rotation. The top edge is subjected to a rotation of $\pi/4$ with respect to its center and around axis 3 and to an additional translation $U_1 = 2$ in direction 1. The micro-rotation at the top is set to 1. This results in combined shear and flexion loading conditions. The deformed states for the reference composite material and for a homogeneous medium HS2 are given on Fig. 8. A quantitative comparison between the HS1 and HS2 predictions and the actual response of the heterogeneous material is given on Fig. 9. The predictions of the displacement field coincide for the homogenization schemes 1 and 3. However, HS2 turns out to give a slightly better approximation of the actual fields ($l_c/l = 1$). The Cauchy continuum still provides a fair estimation of the actual response for this type of loading conditions. The procedure HS3 leads to a solution close to that of HS2.

6. Conclusions

It has been shown that a heterogeneous Cosserat medium can be replaced by a homogeneous Cauchy continuum when the characteristic lengths l and l_c are comparable and much smaller than the size L of the structure, and by a homogeneous Cosserat continuum when l_c is of the order of L. The numerical simulations have confirmed this hierarchy. Furthermore, they indicate that a Cosserat effective medium can still be relevant when l, l_c and L all have the same order of magnitude. This corresponds to a frequent situation in practical structural applications, where the size of the heterogeneities is not negligible when compared to the size of the structure. It can be noted that the Cauchy part of the effective properties obtained according to HS1 and HS2 are slightly different, as can be seen from Tables 2 and 3. An important feature in the analysis of composite structures has not been taken into account in this work, namely the existence of boundary effects that may play a significant role in stress–strain distributions in structures like those computed in Section 4. Special attention should be paid to the analysis of some boundary layers, as it is done in the classical case (Dumontet, 1990).

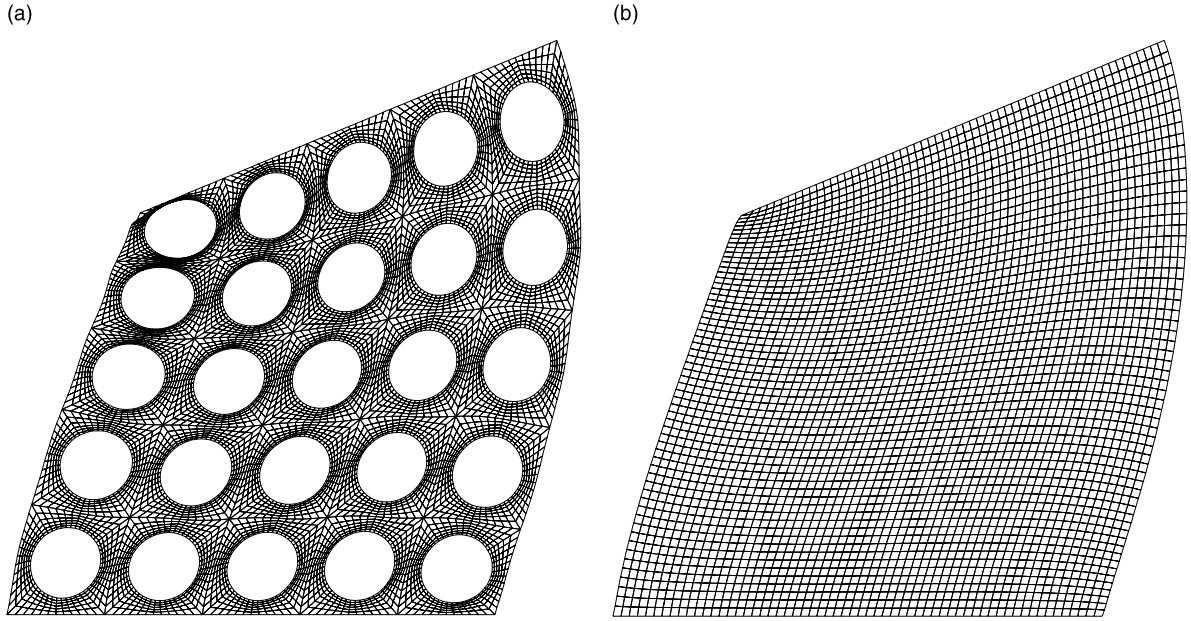

Fig. 8. Combined shear and flexion on (a) a fiber matrix composite with $l_c/l = 1$ (left, the mesh of the fibers has not been represented; mesh deformation has been strongly magnified for the illustration) and (b) on the homogeneous equivalent medium according to HS2 (right).

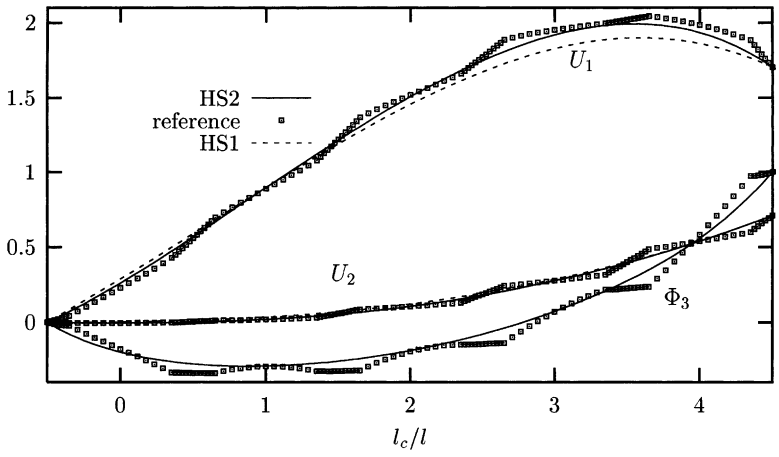

Fig. 9. Comparison of the displacements and micro-rotation along a vertical line in the middle of the fourth row, given by the reference calculation and the homogeneous equivalent media according to HS1 and HS2 ($l_c/l = 1$): U_1/l, U_2/l and Φ_3 from top to bottom (Φ_3 cannot be plotted for HS1).

The results presented in this work have found two main applications. It has been used firstly by Pradel and Sab (1998) for the homogenization of discrete media like beam networks or foams. For, the authors have shown that such discrete media can be embedded in the Cosserat continuum and the previous results can be directly used to derive the effective properties of discrete heterogeneous media. According to the ratio of the bending stiffness to Young's modulus and the length of each beam of a truss, the effective

medium can be a Cauchy or a Cosserat medium. The second application deals with non-linear properties of crystals. In Forest (1998), single crystals are regarded as Cosserat materials. As a result, a polycrystal becomes a heterogeneous Cosserat material and the homogenization scheme, HS1 has been used by Forest et al. (2000) to predict the effect of grain size on polycrystal yielding.

Appendix A. Resolution of the homogenization problem HS1

The resolution method proposed here mainly follows the lines of Boutin (1996). We first define three differential operators L_c^{-2}, L_c^{-1} and L_c^0:

$$L_c^{-i}\begin{pmatrix}\underline{\mathbf{u}}\\ \underline{\boldsymbol{\phi}}\end{pmatrix}=\begin{bmatrix}L_{c1}^{-i}\\ L_{c2}^{-i}\end{bmatrix}\begin{pmatrix}\underline{\mathbf{u}}\\ \underline{\boldsymbol{\phi}}\end{pmatrix} \tag{A.1}$$

for $i\in\{0,1,2\}$. The components of these operators read

$$L_{c1}^{-2}\begin{pmatrix}\underline{\mathbf{u}}\\ \underline{\boldsymbol{\phi}}\end{pmatrix}=\left[\underset{\approx}{\mathbf{a}}^{(0)}:(\underline{\mathbf{u}}\otimes\underline{\nabla}_y+\underset{\approx}{\boldsymbol{\epsilon}}\cdot\underline{\boldsymbol{\phi}})\right]\cdot\underline{\nabla}_y,$$

$$L_{c2}^{-2}\begin{pmatrix}\underline{\mathbf{u}}\\ \underline{\boldsymbol{\phi}}\end{pmatrix}=\left[\underset{\approx}{\mathbf{c}}:\underline{\boldsymbol{\phi}}\otimes\underline{\nabla}_y\right]\cdot\underline{\nabla}_y-\underset{\approx}{\boldsymbol{\epsilon}}:\left[\underset{\approx}{\mathbf{a}}^{(0)}:(\underline{\mathbf{u}}\otimes\underline{\nabla}_y+\underset{\approx}{\boldsymbol{\epsilon}}\cdot\underline{\boldsymbol{\phi}})\right], \tag{A.2}$$

$$L_{c1}^{-1}\begin{pmatrix}\underline{\mathbf{u}}\\ \underline{\boldsymbol{\phi}}\end{pmatrix}=\left[\underset{\approx}{\mathbf{a}}^{(0)}:\underline{\mathbf{u}}\otimes\underline{\nabla}_x\right]\cdot\underline{\nabla}_y+\left[\underset{\approx}{\mathbf{a}}^{(0)}:(\underline{\mathbf{u}}\otimes\underline{\nabla}_y+\underset{\approx}{\boldsymbol{\epsilon}}\cdot\underline{\boldsymbol{\phi}})\right]\cdot\underline{\nabla}_x,$$

$$L_{c2}^{-1}\begin{pmatrix}\underline{\mathbf{u}}\\ \underline{\boldsymbol{\phi}}\end{pmatrix}=\left[\underset{\approx}{\mathbf{c}}^{(1)}:\underline{\boldsymbol{\phi}}\otimes\underline{\nabla}_y\right]\cdot\underline{\nabla}_y+\left[\underset{\approx}{\mathbf{c}}^{(1)}:\underline{\boldsymbol{\phi}}\otimes\underline{\nabla}_y\right]\cdot\underline{\nabla}_x-\underset{\approx}{\boldsymbol{\epsilon}}:(\underset{\approx}{\mathbf{a}}^{(0)}:\underline{\mathbf{u}}\otimes\underline{\nabla}_x), \tag{A.3}$$

$$L_{c1}^{0}\begin{pmatrix}\underline{\mathbf{u}}\\ \underline{\boldsymbol{\phi}}\end{pmatrix}=(\underset{\approx}{\mathbf{a}}^{(0)}:\underline{\mathbf{u}}\otimes\underline{\nabla}_x)\cdot\underline{\nabla}_x,\qquad L_{c2}^{0}\begin{pmatrix}\underline{\mathbf{u}}\\ \underline{\boldsymbol{\phi}}\end{pmatrix}=\left[\underset{\approx}{\mathbf{c}}^{(1)}:\underline{\boldsymbol{\phi}}\otimes\underline{\nabla}_x\right]\cdot\underline{\nabla}_x. \tag{A.4}$$

Using these operators, the auxiliary problems (27), (29) and (30) can be rewritten in a concise manner:

$$\begin{aligned}
&L_c^{-2}\begin{pmatrix}\underline{\mathbf{u}}_0\\ 0\end{pmatrix}=0,\\
&L_c^{-2}\begin{pmatrix}\underline{\mathbf{u}}_1\\ \underline{\boldsymbol{\phi}}_1\end{pmatrix}=-L_c^{-1}\begin{pmatrix}\underline{\mathbf{u}}_0\\ 0\end{pmatrix}-\begin{vmatrix}0\\ \underline{\mathbf{c}}\end{vmatrix},\\
&L_c^{-2}\begin{pmatrix}\underline{\mathbf{u}}_2\\ \underline{\boldsymbol{\phi}}_2\end{pmatrix}=-L_c^{-1}\begin{pmatrix}\underline{\mathbf{u}}_1\\ \underline{\boldsymbol{\phi}}_1\end{pmatrix}-L_c^{0}\begin{pmatrix}\underline{\mathbf{u}}_0\\ 0\end{pmatrix}-\begin{vmatrix}\underline{\mathbf{f}}\\ 0\end{vmatrix}.
\end{aligned} \tag{A.5}$$

To solve these problems, the kernel of the operator L_c^{-2} must be studied. This amounts to solving the following general problem:

$$L_c^{-2}\begin{pmatrix}\underline{\mathbf{u}}\\ \underline{\boldsymbol{\phi}}\end{pmatrix}(\underline{\mathbf{x}},\underline{\mathbf{y}})=\begin{bmatrix}\underline{\mathbf{g}}\\ \underline{\mathbf{h}}\end{bmatrix}(\underline{\mathbf{x}},\underline{\mathbf{y}}), \tag{A.6}$$

where the unknowns $\underline{\mathbf{u}}$ and $\underline{\boldsymbol{\phi}}$ are elements of the space $\mathscr{V}_{\text{per}}$ of Y-periodic fields. The vector fields $\underline{\mathbf{g}}$ and $\underline{\mathbf{h}}$ are also assumed to be Y-periodic. The weak formulation of the previous problem amounts to finding out $\underline{\mathbf{u}}$, $\underline{\boldsymbol{\phi}}$ in $\mathscr{V}_{\text{per}}$ such that

$$\forall \hat{\underline{\mathbf{u}}}, \hat{\underline{\boldsymbol{\phi}}}\ Y\text{-periodic}, \qquad \int_Y \left(L_{c1}^{-2}\begin{pmatrix} \underline{\mathbf{u}} \\ \underline{\boldsymbol{\phi}} \end{pmatrix} \cdot \hat{\underline{\mathbf{u}}} + L_{c2}^{-2}\begin{pmatrix} \underline{\mathbf{u}} \\ \underline{\boldsymbol{\phi}} \end{pmatrix} \cdot \hat{\underline{\boldsymbol{\phi}}} \right) \mathrm{d}\omega_y = \int_Y \left(\underline{\mathbf{g}} \cdot \hat{\underline{\mathbf{u}}} + \underline{\mathbf{h}} \cdot \hat{\underline{\boldsymbol{\phi}}} \right) \mathrm{d}\omega_y, \tag{A.7}$$

where all terms are functions of $\underline{\mathbf{x}}$ and $\underline{\mathbf{y}}$. After integrating by parts and taking the Y-periodicity into account, the formulation is equivalent to

$$\int_Y \left[\underset{\sim}{\mathbf{e}}_y\begin{pmatrix} \underline{\mathbf{u}} \\ \underline{\boldsymbol{\phi}} \end{pmatrix} : \underset{\approx}{\mathbf{a}}^{(0)} : \underset{\sim}{\mathbf{e}}_y\begin{pmatrix} \hat{\underline{\mathbf{u}}} \\ \hat{\underline{\boldsymbol{\phi}}} \end{pmatrix} + \underset{\sim}{\boldsymbol{\kappa}}_y\begin{pmatrix} \hat{\underline{\mathbf{u}}} \\ \hat{\underline{\boldsymbol{\phi}}} \end{pmatrix} : \underset{\approx}{\mathbf{c}}^{(1)} : \underset{\sim}{\boldsymbol{\kappa}}_y\begin{pmatrix} \underline{\mathbf{u}} \\ \underline{\boldsymbol{\phi}} \end{pmatrix} \right] \mathrm{d}\omega_y = -\int_Y \left(\underline{\mathbf{g}} \cdot \hat{\underline{\mathbf{u}}} + \underline{\mathbf{h}} \cdot \hat{\underline{\boldsymbol{\phi}}} \right) \mathrm{d}\omega_y \tag{A.8}$$

for all Y-periodic fields $(\hat{\underline{\mathbf{u}}}, \hat{\underline{\boldsymbol{\phi}}})$ and

$$\underset{\sim}{\mathbf{e}}_y\begin{pmatrix} \underline{\mathbf{u}} \\ \underline{\boldsymbol{\phi}} \end{pmatrix} = \underline{\mathbf{u}} \otimes \underline{\nabla}_y + \underset{\approx}{\boldsymbol{\epsilon}} \cdot \underline{\boldsymbol{\phi}}, \qquad \underset{\sim}{\boldsymbol{\kappa}}_y\begin{pmatrix} \underline{\mathbf{u}} \\ \underline{\boldsymbol{\phi}} \end{pmatrix} = \underline{\boldsymbol{\phi}} \otimes \underline{\nabla}_y$$

are the strain operators for a Cosserat medium. The right-hand side of Eq. (A.8) is a scalar product on $\mathscr{V}_{\mathrm{per}}/\mathscr{R}_{\mathrm{per}}$, $\mathscr{R}_{\mathrm{per}}$ being the space of constant translation fields. As a result, an equivalent formulation of the problem is to look for the minimum of

$$\frac{1}{2}\int_Y \left[\underset{\sim}{\mathbf{e}}_y^{\mathrm{T}}\begin{pmatrix} \underline{\mathbf{u}} \\ \underline{\boldsymbol{\phi}} \end{pmatrix} : \underset{\approx}{\mathbf{a}}^{(0)} : \underset{\sim}{\mathbf{e}}_y\begin{pmatrix} \underline{\mathbf{u}} \\ \underline{\boldsymbol{\phi}} \end{pmatrix} + \underset{\sim}{\boldsymbol{\kappa}}_y^{\mathrm{T}}\begin{pmatrix} \underline{\mathbf{u}} \\ \underline{\boldsymbol{\phi}} \end{pmatrix} : \underset{\approx}{\mathbf{c}}^{(1)} : \underset{\sim}{\boldsymbol{\kappa}}_y\begin{pmatrix} \underline{\mathbf{u}} \\ \underline{\boldsymbol{\phi}} \end{pmatrix} \right] \mathrm{d}\omega_y + \int_Y \left(\underline{\mathbf{g}} \cdot \underline{\mathbf{u}} + \underline{\mathbf{h}} \cdot \underline{\boldsymbol{\phi}} \right) \mathrm{d}\omega_y \tag{A.9}$$

provided that the linear form

$$r\begin{pmatrix} \underline{\mathbf{u}} \\ \underline{\boldsymbol{\phi}} \end{pmatrix} = \int_Y \underline{\mathbf{g}} \cdot \underline{\mathbf{u}} + \underline{\mathbf{h}} \cdot \underline{\boldsymbol{\phi}}\, \mathrm{d}\omega_y$$

is orthogonal (in terms of duality) to $\mathscr{R}_{\mathrm{per}}$, which means

$$\forall \underline{\mathbf{U}} \in R^3, \quad r\begin{pmatrix} \underline{\mathbf{U}} \\ 0 \end{pmatrix} = 0.$$

The previous condition of orthogonality is therefore equivalent to $\langle \underline{\mathbf{g}} \rangle = 0$. This leads to the following lemma.

Lemma 1. (*inversion of L_c^{-2} for HS1*). *Given two fields* $\underline{\mathbf{g}}$ *and* $\underline{\mathbf{h}}$ Y*-periodic, the equation,*

$$L_c^{-2}\begin{pmatrix} \underline{\mathbf{u}} \\ \underline{\boldsymbol{\phi}} \end{pmatrix} = \begin{bmatrix} \underline{\mathbf{g}} \\ \underline{\mathbf{h}} \end{bmatrix} \tag{A.10}$$

admits a unique solution up to a constant translation field, if and only if,

$$\left\langle \underline{\mathbf{g}} \right\rangle = 0. \tag{A.11}$$

Let us apply this lemma to Eq. (A.5). The conditions

$$\begin{aligned} &\left\langle L_{c1}^{-1}\begin{pmatrix} \underline{\mathbf{U}}_0 \\ 0 \end{pmatrix} \right\rangle = 0, \\ &\left\langle L_{c1}^{-1}\begin{pmatrix} \underline{\mathbf{u}}_1 \\ \underline{\boldsymbol{\phi}}_1 \end{pmatrix} \right\rangle + \left\langle L_{c1}^{0}\begin{pmatrix} \underline{\mathbf{U}}_0 \\ 0 \end{pmatrix} \right\rangle + \underline{\mathbf{f}} = \underset{\sim}{\boldsymbol{\Sigma}}_0 \cdot \underline{\nabla} + \underline{\mathbf{f}} = 0 \end{aligned} \tag{A.12}$$

are identically fulfilled, so that the problem (A.5) admits a unique solution explicited in Section 3.3.

Appendix B. Resolution of the homogenization problem HS2

According to HS2, the linear operators introduced in Appendix A are slightly modified:

$$L_{c1}^{-2}\begin{pmatrix}\underline{\mathbf{u}}\\ \underline{\boldsymbol{\phi}}\end{pmatrix}=\left[\underset{\approx}{\mathbf{a}}^{(0)}:\underline{\mathbf{u}}\otimes\underline{\nabla}_y\right]\cdot\underline{\nabla}_y,\qquad L_{c2}^{-2}\begin{pmatrix}\underline{\mathbf{u}}\\ \underline{\boldsymbol{\phi}}\end{pmatrix}=\left[\underset{\approx}{\mathbf{c}}^{(2)}:\underline{\boldsymbol{\phi}}\otimes\underline{\nabla}_y\right]\cdot\underline{\nabla}_y, \tag{B.1}$$

$$\begin{aligned}L_{c1}^{-1}\begin{pmatrix}\underline{\mathbf{u}}\\ \underline{\boldsymbol{\phi}}\end{pmatrix}&=\left[\underset{\approx}{\mathbf{a}}^{(0)}:(\underline{\mathbf{u}}\otimes\underline{\nabla}_x+\underset{\simeq}{\boldsymbol{\epsilon}}\cdot\underline{\boldsymbol{\phi}})\right]\cdot\underline{\nabla}_y+\left[\underset{\approx}{\mathbf{a}}^{(0)}:\underline{\mathbf{u}}\otimes\underline{\nabla}_y\right]\cdot\underline{\nabla}_x,\\ L_{c2}^{-1}\begin{pmatrix}\underline{\mathbf{u}}\\ \underline{\boldsymbol{\phi}}\end{pmatrix}&=\left[\underset{\approx}{\mathbf{c}}^{(2)}:\underline{\boldsymbol{\phi}}\otimes\underline{\nabla}_y\right]\cdot\underline{\nabla}_y+\left[\underset{\approx}{\mathbf{c}}^{(2)}:\underline{\boldsymbol{\phi}}\otimes\underline{\nabla}_y\right]\cdot\underline{\nabla}_x-\underset{\simeq}{\boldsymbol{\epsilon}}:\left[\underset{\approx}{\mathbf{a}}^{(0)}(\underline{\mathbf{y}}):\underline{\mathbf{u}}\otimes\underline{\nabla}_y\right],\end{aligned} \tag{B.2}$$

$$\begin{aligned}L_{c1}^{0}\begin{pmatrix}\underline{\mathbf{u}}\\ \underline{\boldsymbol{\phi}}\end{pmatrix}&=\left[\underset{\approx}{\mathbf{a}}^{(0)}:(\underline{\mathbf{u}}\otimes\underline{\nabla}_x+\underset{\simeq}{\mathbf{e}}\cdot\underline{\boldsymbol{\phi}})\right]\cdot\underline{\nabla}_{\mathbf{x}},\\ \mathbf{L}_{c2}^{0}\begin{pmatrix}\underline{\mathbf{u}}\\ \underline{\boldsymbol{\phi}}\end{pmatrix}&=\left[\underset{\approx}{\mathbf{c}}^{(2)}:\underline{\boldsymbol{\phi}}\otimes\underline{\nabla}_{\mathbf{x}}-\underset{\simeq}{\boldsymbol{\epsilon}}:(\underset{\approx}{\mathbf{a}}^{(0)}(\underline{\mathbf{y}}):\underline{\mathbf{u}}\otimes\underline{\nabla}_{\mathbf{x}})\right]\cdot\underline{\nabla}_{\mathbf{x}}.\end{aligned} \tag{B.3}$$

The auxiliary problems (37), (39) and (40) can be rewritten in a concise form:

$$\begin{aligned}&L_c^{-2}\begin{pmatrix}\underline{\mathbf{U}}_0,\\ \underline{\boldsymbol{\Phi}}_1\end{pmatrix}=0,\\ &L_c^{-2}\begin{pmatrix}\underline{\mathbf{u}}_1\\ \underline{\boldsymbol{\phi}}_2\end{pmatrix}+L_c^{-1}\begin{pmatrix}\underline{\mathbf{U}}_0,\\ \underline{\boldsymbol{\Phi}}_1\end{pmatrix}=0,\\ &L_c^{-2}\begin{pmatrix}\underline{\mathbf{u}}_2\\ \underline{\boldsymbol{\phi}}_3\end{pmatrix}+L_c^{-1}\begin{pmatrix}\underline{\mathbf{u}}_1\\ \underline{\boldsymbol{\phi}}_2\end{pmatrix}+L_c^{0}\begin{pmatrix}\underline{\mathbf{U}}_0\\ \underline{\boldsymbol{\Phi}}_1\end{pmatrix}+\begin{vmatrix}\underline{\mathbf{f}}\\ \underline{\mathbf{c}}\end{vmatrix}=0.\end{aligned} \tag{B.4}$$

In this case, the kernel $\mathscr{R}_{\text{per}}$ of the new operator L_c^{-2} is the space of constant translations and micro-rotations. We establish the following lemma.

Lemma 2. (*inversion of L_c^{-2} for HS2*). *Given two fields* $\underline{\mathbf{g}}$ *and* $\underline{\mathbf{h}}$ *Y-periodic, the equation,*

$$L_c^{-2}\begin{pmatrix}\underline{\mathbf{u}}\\ \underline{\boldsymbol{\phi}}\end{pmatrix}=\begin{bmatrix}\underline{\mathbf{g}}\\ \underline{\mathbf{h}}\end{bmatrix} \tag{B.5}$$

admits a unique solution up to constant fields $(\underline{\mathbf{u}},\underline{\boldsymbol{\phi}})$, *if and only if,*

$$\langle\underline{\mathbf{g}}\rangle=0,\quad\langle\underline{\mathbf{h}}\rangle=0. \tag{B.6}$$

These conditions are identically fulfilled in the case of problem (B.4) and the final solution is explicited in Section 3.5.

References

Aifantis, E.C., 1992. On the role of gradients in the localization of deformation and fracture. International Journal of Engineering Science 30, 1279–1299.

Ashby, M.F., 1971. The deformation of plastically non-homogeneous alloys. In: Kelly, A., Nicholson, R.B. (Eds.), Strengthening Methods in Crystals. Applied Science Publishers, London, pp. 137–192.

Besson, J., Foerch, R., 1997. Large scale object-oriented finite element code design. Computer Methods in Applied Mechanics and Engineering 142, 165–187.

Besson, J., Bultel, F., Forest, S., 1999. Plasticité des milieux de Cosserat: application aux composites particulaires. In: 4ème Colloque en Calcul des Structures, Teknea, Toulouse, pp. 759–764.

Boutin, C., 1996. Micro-structural effects in elastic composites. International Journal of Solids and Structures 33, 1023–1051.

Dai, H., Parks, D.M., 1998. Geometrically-necessary dislocation density and scale-dependent crystal plasticity. In: Khan, A.S. (Ed.), Proceedings of Plasticity '97. Neat Press, Fulton, Maryland, pp. 17–18.

De Borst, R., 1991. Simulation of strain localization: a reappraisal of the Cosserat continuum. Engineering Computations 8, 317–332.

Dumontet, H., 1990. Homogénéisation et effets de bords dans les matériaux composites. Doctoral thesis, University P. et M., Curie, Paris.

Eringen, A.C., 1976. Polar and non local field theories. Continuum Physics, vol. 4. Academic Press, New York.

Forest, S., 1998. Modeling slip, kink and shear banding in classical and generalized single crystal plasticity. Acta Materialia 46 (9), 3265–3281.

Forest, S., Sab, K., 1998. Overall modelling of periodic heterogeneous Cosserat media. In: Inan, E., Markov, K.Z. (Eds.), Ninth International Symposium on Continuum Models and Discrete Systems. World Scientific, Singapore, pp. 445–453.

Forest, S., Barbe, F., Cailletaud, G., 2000. Cosserat modelling of size effects in the mechanical behavior of polycrystals and multiphase materials, submitted for publication.

Forest, S., Dendievel, R., Canova, G., 1999. Estimating the overall properties of heterogeneous Cosserat materials. Modelling and Simulation in Materials Science and Engineering 7 (5), 829–840.

Gambin, B., Kröner, E., 1989. Higher order terms in the homogenized stress–strain relation of periodic elastic media. Physica Status Solidi B 151, 513–519.

Ilcewicz, L.B., Narasimhan, M.N.L, Wilson, J.B., 1986. Micro and macro-material symmetries in generalized continua. International Journal of Engineering 24, 97–109.

Pradel, F., 1998. Homogénéisation des milieux continus et discrets périodiques orientés. Une application aux mousses. Doctoral Thesis, Ecole Nationale des Ponts et Chaussées.

Pradel, F., Sab, K., 1998. Homogenization of discrete media. Journal de Physique IV France, 8, Pr8-317–324.

Smyshlyaev, V.P., Fleck, N.A., 1994. Bounds and estimates for linear composites with strain gradient effects. Journal of the Mechanics and Physics of Solids 42, 1851–1882.

Smyshlyaev, V.P., Fleck, N.A., 1996. The role of strain gradients in the grain size effect for polycrystals. Journal of the Mechanics and Physics of Solids 44, 465–495.

Sanchez-Palencia, E., 1974. Comportement local et macroscopique d'un type de milieux physiques hétérogènes. International Journal of Engineering Science 12, 331–351.

Sanchez-Palencia, E., Zaoui, A., 1985. Homogenization techniques for composite media. Lecture Notes in Physics, vol. 272. Springer, Berlin.

Suquet, P., 1997. Continuum Micro-mechanics, CISM Courses and Lectures no. 397, Springer, Berlin.

Triantafyllidis, N., Bardenhagen, S., 1996. The influence of scale size on the stability of periodic solids and the role of associated higher order gradient continuum models. Journal of the Mechanics and Physics of Solids 44, 1891–1928.

Zhu, H.T., Zbib, H.M., Aifantis, E.C., 1997. Strain gradients and continuum modeling of size effect in metal matrix composites. Acta Mechanica 121, 165–176.